Naval Research Laboratory
Washington, DC 20375-5000

NRL Report 9110

Automatic Detection, Tracking, and Sensor Integration

G. V. TRUNK

Radar Analysis Branch
Radar Division

June 8, 1988

SECURITY CLASSIFICATION OF THIS PAGE

REPORT DOCUMENTATION PAGE

Form Approved
OMB No. 0704-0188

1a REPORT SECURITY CLASSIFICATION UNCLASSIFIED	1b RESTRICTIVE MARKINGS
2a SECURITY CLASSIFICATION AUTHORITY	3 DISTRIBUTION/AVAILABILITY OF REPORT Approved for public release; distribution unlimited.
2b DECLASSIFICATION/DOWNGRADING SCHEDULE	
4 PERFORMING ORGANIZATION REPORT NUMBER(S) NRL Report 9110	5 MONITORING ORGANIZATION REPORT NUMBER(S)
6a NAME OF PERFORMING ORGANIZATION Naval Research Laboratory 6b OFFICE SYMBOL (If applicable) Code 5310	7a NAME OF MONITORING ORGANIZATION
6c ADDRESS (City, State, and ZIP Code) Washington, DC 20375-5000	7b ADDRESS (City, State, and ZIP Code)
8a NAME OF FUNDING/SPONSORING ORGANIZATION Office of Naval Research 8b OFFICE SYMBOL (If applicable)	9 PROCUREMENT INSTRUMENT IDENTIFICATION NUMBER
8c ADDRESS (City, State, and ZIP Code) Arlington, VA 22217	10 SOURCE OF FUNDING NUMBERS PROGRAM ELEMENT NO: 61153N; PROJECT NO: DN480-006; TASK NO: RR021-05-43; WORK UNIT ACCESSION NO: 53-0626-00
11 TITLE (Include Security Classification) Automatic Detection, Tracking, and Sensor Integration	
12 PERSONAL AUTHOR(S) Trunk G.V.	
13a TYPE OF REPORT Interim 13b TIME COVERED FROM _____ TO _____ 14 DATE OF REPORT (Year, Month, Day) 1988 June 8 15 PAGE COUNT 61	
16 SUPPLEMENTARY NOTATION	

17 COSATI CODES			18 SUBJECT TERMS (Continue on reverse if necessary and identify by block number)		
FIELD	GROUP	SUB-GROUP	Automatic detection	Adaptive thresholds	Track-while scan
			Detectors	Clutter map	Sensor integration
			CFAR	Automatic tracking	

19 ABSTRACT (Continue on reverse if necessary and identify by block number)

This report surveys the state of the art of automatic detection, tracking, and sensor integration. In the area of detection, various noncoherent integrators such as the moving window integrator, feedback integrator, two-pole filter, binary integrator, and batch processor are discussed. Next, the three techniques for controlling false alarms, adapting thresholds, nonparametric detectors, and clutter maps are presented. In the area of tracking, a general outline is given of a track-while-scan system, and then a discussion is presented of the file system, contact-entry logic, coordinate systems, tracking filters, maneuver-following logic, tracking initiation, track-drop logic, and correlation procedures. Finally, in the area of multisensor integration the problems of colocated-radar integration, multisite-radar integration, radar-IFF integration, and radar-DF bearing strobe integration are treated.

20 DISTRIBUTION/AVAILABILITY OF ABSTRACT ☒ UNCLASSIFIED/UNLIMITED ☐ SAME AS RPT ☐ DTIC USERS	21 ABSTRACT SECURITY CLASSIFICATION UNCLASSIFIED
22a NAME OF RESPONSIBLE INDIVIDUAL G. V. Trunk	22b TELEPHONE (Include Area Code) (202) 767-2573 22c OFFICE SYMBOL Code 5310

DD Form 1473, JUN 86

SECURITY CLASSIFICATION OF THIS PAGE

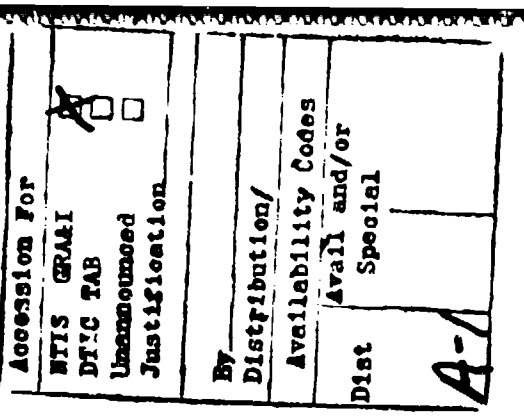

CONTENTS

AUTOMATIC DETECTION, TRACKING, AND SENSOR INTEGRATION

INTRODUCTION

Since the invention of radar, radar operators have detected and tracked targets by using visual inputs from a variety of displays. Although operators can perform these tasks very accurately, they are easily saturated and quickly become fatigued. Various studies have shown that operators can manually track only two to four targets. To correct this situation, automatic detection and tracking (ADT) systems were attached to many radars. Undoubtedly, as digital processing increases in speed, and hardware decreases in cost and size, ADT systems will become associated with almost all but the simplest radars.

This report discusses automatic detection, automatic tracking, and sensor integration systems for air-surveillance radar. Included in this discussion are various noncoherent integrators that provide target enhancement, thresholding techniques for reducing false alarms and target suppression, and algorithms for estimating target position and resolving targets. Then, an overview is given of the entire tracking system followed by a discussion of its various components such as tracking filter, maneuver-following logic, track initiation, and correlation logic. Next, multiscan approaches to automatic tracking such as maximum likelihood are discussed. Finally, the report concludes with a discussion of sensor integration and radar netting, including colocated and multisite systems.

AUTOMATIC DETECTION

In the 1940s, Marcum [1] introduced to the radar community the statistical framework necessary for the development of automatic detection. Later, Swerling [2] extended the work to fluctuating targets. They investigated many of the statistical problems associated with the noncoherent detection of targets in Rayleigh noise. The most important result of the investigation was the generation of curves of probability of detection (P_D) vs signal-to-noise ratio (S/N) for a detector that sums N enveloped-detected samples (either linear or square law) under the assumption of equal signal amplitudes. However, in a search radar, as the beam sweeps over the target, the returned signal amplitude is modulated by the antenna pattern. Many authors investigated various detectors (weightings), comparing detection performance and angular estimation results to the optimal values.

In the original work on these detectors, the environment was assumed to be known and homogeneous so that fixed thresholds could be used. However, a realistic environment (e.g., containing land, sea, and rain) will cause an exorbitant number of false alarms for a fixed threshold system that does not use excellent coherent processing; therefore, three main approaches, adaptive thresholding, nonparametric detectors, and clutter maps were used to solve the false-alarm problem. Adaptive thresholding and nonparametric detectors are based on the assumption that homogeneity exists in a small region about the range cell that is being tested. The adaptive thresholding method assumes that the noise density is known except for a few unknown parameters (e.g., the mean and variance). The surrounding reference cells are then used to estimate the unknown parameters, and a threshold is obtained based on the estimated density. Nonparametric detectors obtain a constant false-alarm rate

Manuscript approved December 23, 1987.

(CFAR) by ranking (i.e., ordering the samples from smallest to largest) the test samples, usually with the reference cells. Under the hypothesis that all the samples (test and reference) are independent samples from an unknown density function, the test sample has a uniform density function; consequently a threshold that yields CFAR can be set. Clutter maps store an average background level for each range-azimuth cell. A target is then declared in a range-azimuth cell if the new value exceeds the average background level by a specified amount.

Optimal Detector

The radar-detection problem is a binary hypothesis testing problem

H_0: No target present

H_1: Target present.

Several criteria (i.e., definitions of optimality) can be used to solve this problem, but the most appropriate for radar is the Neyman-Pearson [3]. This criterion maximizes the P_D for a given probability of false alarm P_{fa} by comparing the likelihood of ratio L to an appropriate threshold T. A target is declared present if

$$L(x_1, \ldots, x_n) = \frac{p(x_1, \ldots, x_n \mid H_1)}{p(x_1, \ldots, x_n \mid H_0)} \geq T, \tag{1}$$

where $p(x_1, \ldots, x_n \mid H_1)$ and $P(x_1, \ldots, x_n \mid H_0)$ are the joint densities of the n samples x_i under the conditions of target presence and target absence respectively. For a linear envelope detector the samples have a Rayleigh density under H_0 and a Ricean density under H_1, and the likelihood detector reduces to

$$\sum_{i=1}^{n} I_0 \left(\frac{A_i x_i}{\sigma^2} \right) \geq T, \tag{2}$$

where I_0 is the Bessel function of zero order, σ^2 is the noise power, and A_i is the target amplitude on the ith pulse and is proportional to the power antenna pattern. For small signals ($A_i << \sigma$), the detector reduces to the square-law detector:

$$\sum_{i=1}^{n} A_i^2 x_i^2 \geq T. \tag{3}$$

For $A_i = A$, this detector and the linear detector were studied first by Marcum [1] and in the succeeding years by numerous other people. The most important facts concerning these detectors are as follows:

- The detection performances of the linear and square-law detectors are similar. The difference is less than 0.2 dB over wide ranges of P_D, P_{fa}, and n.

- Since the signal return of a scanning radar is modulated by the antenna pattern, to maximize the S/N only 0.84 of the pulses between the half-power points should be integrated, and the antenna

beam shape factor (ABSF) is 1.6 dB [4]. The ABSF is the number by which the midbeam S/N must be reduced so that the detection curves generated for equal signal amplitudes can be used for the scanning radar.

• Figure 1 shows that the collapsing loss for the linear detector can be several dB greater than the loss for a square-law detector [5]. The collapsing loss is the additional signal required to maintain the same P_D and P_{fa} when unwanted noise samples along with the desired signal-plus-noise samples are integrated. The number of signal samples integrated is N, the number of extraneous noise samples integrated is M, and the collapsing ratio $\rho = (N + M)/N$.

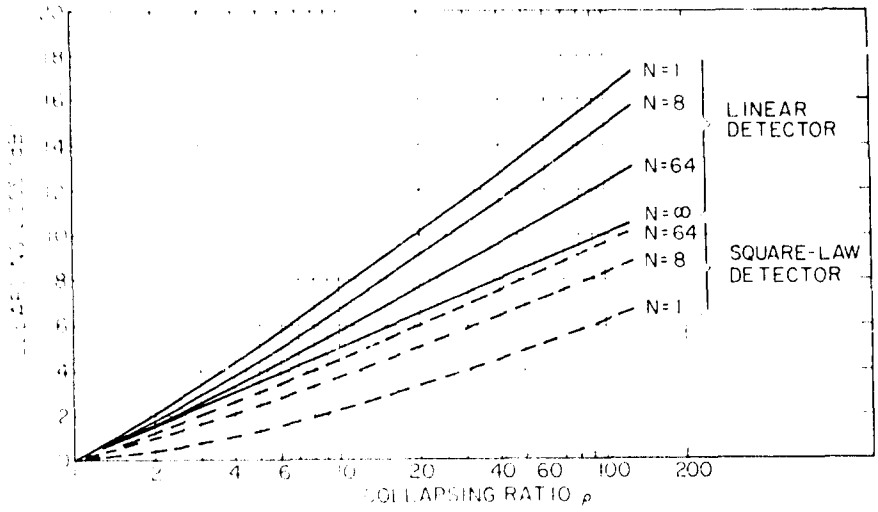

Fig. 1 — Collapsing loss vs collapsing ratio for a probability of false alarm of 10^{-6} and a probability of detection of 0.5, (copyright 1972, IEEE). From G.V. Trunk [5]

Most automatic detectors are required not only to detect targets but to make angular estimates of the azimuth position of the target. Swerling [6] calculated the standard deviation of the optimal estimate by using the Cramer-Rao lower bound. The results are shown in Fig. 2, where a normalized standard deviation is plotted against the midbeam S/N. This result holds for a moderate or large number of pulses integrated, and the optimal estimate involves finding the location where the correlation of the returned signal and the derivative of the antenna pattern is zero. Although this estimate is rarely implemented, its performance is approached by simple estimates.

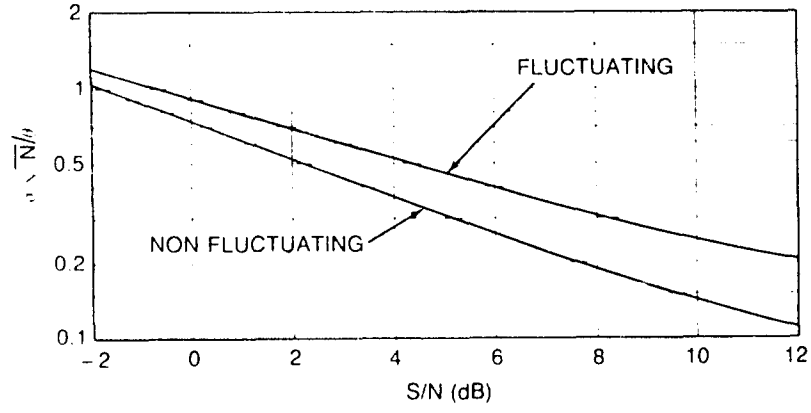

Fig. 2 — Comparison of angular estimates with the Cramer-Rao lower bound. σ is the standard deviation of the estimation error, and N is the number of pulses within the 3 dB beamwidth, which is 2 β/0.85. The S/N is the value at the center of the beam, (copyright 1970, IEEE). From G.V. Trunk [11]

Practical Detectors

Many different detectors are used to accumulate the radar returns as a radar sweeps by a target. Figure 3 shows a few of the most common detectors [7]. Though they are shown as being implemented with shift registers, normally they are implemented with random access memory. The input to these detectors can be either linear, square-law, or log video. Since linear is probably the most commonly used, the advantages and disadvantages of the various detectors will be stated for this video.

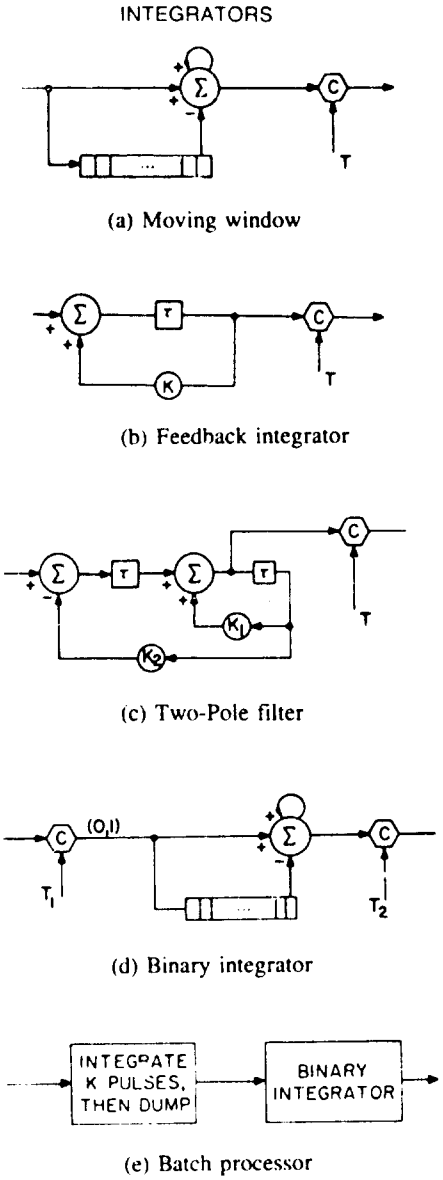

(a) Moving window

(b) Feedback integrator

(c) Two-Pole filter

(d) Binary integrator

(e) Batch processor

Fig. 3 — Block diagrams of various detectors. The letter C indicates a comparison and τ indicates a delay. From G.V. Trunk [7]

Moving Window

The moving window in Fig. 3(a) performs a running sum of n pulses in each range cell;

$$S_i = S_{i-1} + x_i - x_{i-n}, \tag{4}$$

or equivalently,

$$S_i = \sum_{j=0}^{n-1} x_{i-j}, \tag{5}$$

where S_i is the sum on the ith pulse. The performance of this detector is only 0.5 dB worse than the optimal detector given by Eq. (3) [8]. The detection performance can be obtained by using an ABSF of 1.6 dB and the detection curves in Ref. 1. The angular estimate that is obtained by either taking the maximum value of the running sum or by taking the midpoint between the first and last crossing of the detection threshold has a bias of $n/2$ pulses that can be easily corrected. The standard deviation of the estimation error of both estimators is about 20% higher than that for the optimal estimate. The major disadvantage of this detector is its susceptibility to interference; that is, one large sample from interference can cause a detection. A minor disadvantage is that the last n pulses for each range cell must be saved, and therefore a large storage is required when a large number of pulses are integrated. However, because of the availability of large memories of reduced size and cost, this is a minor problem.

The detection performance discussed is based on the assumption that the target is centered in the moving window. In a real situation the radar scans over the target and decisions that are highly correlated are made at every pulse. Hansen [9] analyzed this situation and calculated the detection thresholds shown in Fig. 4, the detection performance shown in Fig. 5, and the angular accuracy shown in Fig. 6. Comparing Hansen's calculation with the single point calculation, one concludes that 1 dB of improvement is obtained by making a decision at every pulse. Figure 6 shows that the angular accuracy of the beam-splitting procedure is about 20% greater than the optimal estimate. For large signal-to-noise ratios, the accuracy (rms error) of the beam-splitting and maximum return procedures will be limited by the pulse spacing [10] and will approach

$$\sigma(\hat{\theta}) = \Delta\theta/\sqrt{12}, \tag{6}$$

where $\Delta\theta$ is the angular rotation between transmitted pulses. Consequently, if the number of pulses per beamwidth is small, the angular accuracy will be poor. For instance, if pulses are separated by 0.5 beamwidth, $\sigma(\hat{\theta})$ is bounded by 0.14 beamwidth. However, improved accuracy can be obtained by using the amplitudes of the radar returns. If one assumes a Gaussian-shaped antenna pattern, an accurate estimate of the target angle is given by

$$\hat{\theta} = \theta_1 + \frac{\Delta\theta}{2} + \frac{1}{2a\,\Delta\theta} \ln(A_2/A_1) \tag{7}$$

where

$$a = 1.386/[\text{beamwidth}]^2, \tag{8}$$

and A_1 and A_2 are the two largest amplitudes of the returned samples and occur at angles θ_1 and $\theta_2 = \theta_1 + \Delta\theta$ respectively. Since the estimate should lie between θ_1 and θ_2 but Eq. (7) will not

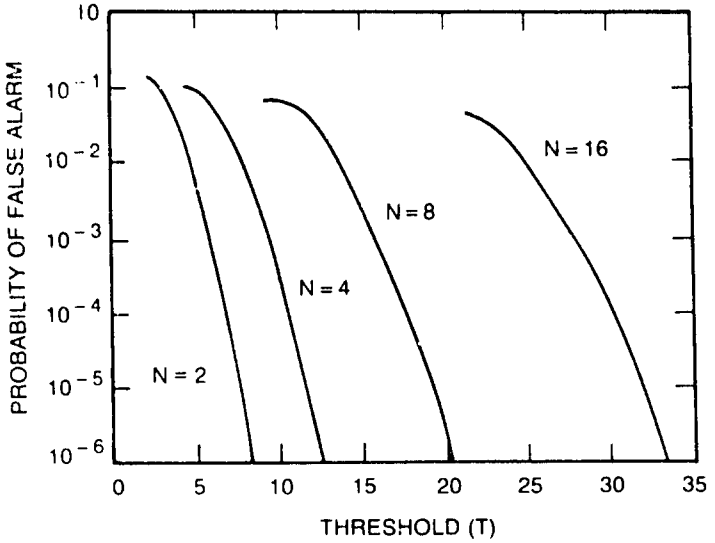

Fig. 4 — Single-sweep false-alarm probability P_{fa} vs threshold for moving window, (copyright 1970, IEEE). From V.G. Hansen [9]

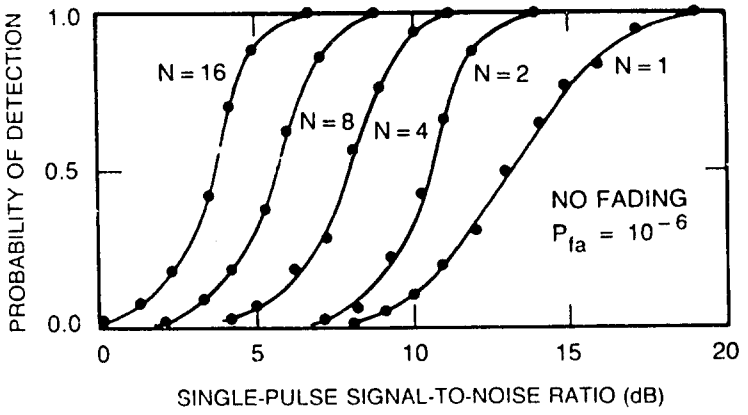

Fig. 5 — Detection performance of the analog moving window detector for the no fading case, (copyright 1970, IEEE). From V.G. Hansen [9]

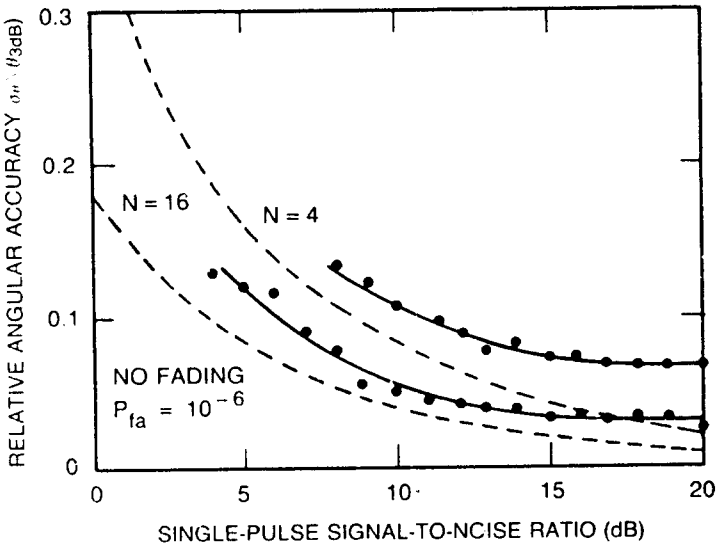

Fig. 6 — Angular accuracy obtained with beam-splitting estimation procedure for the no-fading case. Broken line curves are lower bounds derived by Swerling [6], and points shown are simulation results, (copyright 1970, IEEE). From V.G. Hansen [9]

always yield such as estimate, $\hat{\theta}$ should be set equal to θ_1 if $\hat{\theta} < \theta_1$ and $\hat{\theta}$ should be set equal to θ_2 if $\hat{\theta} > \theta_2$. Figure 7 shows the accuracy of this estimator for the case of $n = 2$ pulses per beamwidth. This estimation procedure can also be used to estimate the elevation angle of a target in multibeam systems.

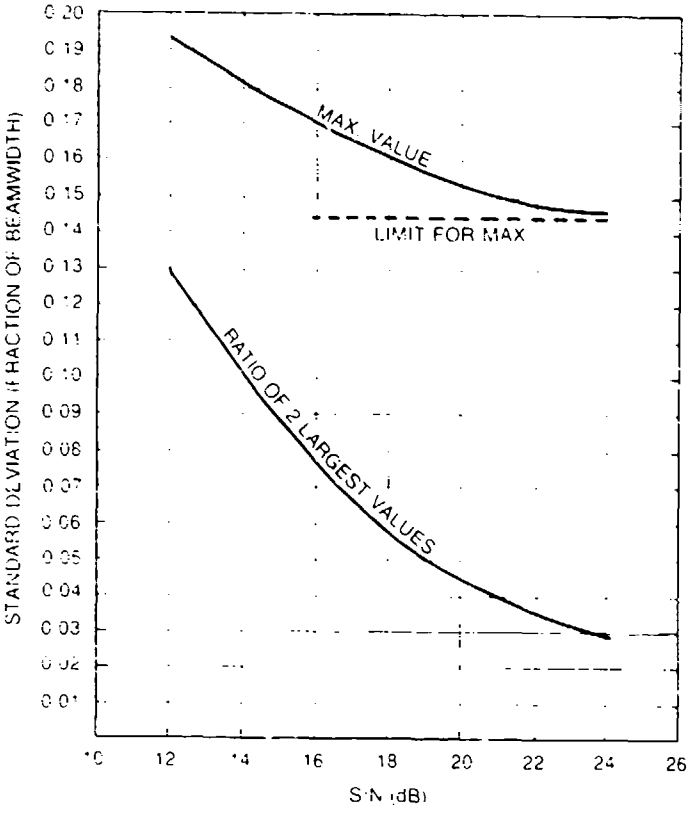

Fig. 7 — Angular accuracy using two-pulse estimates

Feedback Integrator

The amount of storage required can be reduced significantly by using a feedback integrator as shown in Fig. 3(b)

$$s_i = K S_{k-1} + x_i . \tag{9}$$

For a feedback value of K, the effective number of pulse integrated M is $M = 1/(1 - K)$ and for optimal (maximum P_D) performance $M = 0.63$ N, where N is the number of pulses between the 3 dB antenna beamwidth [11]. The detection performance is given by the detection curves for M pulses with ABSF = 1.6 dB [11]. Although the feedback integrator applies an exponential weighting into the past, its detection performance in only 1 dB less than the optimal integrator [8]. However, difficulties are encountered when using the feedback integrator to estimate the azimuth position [11]. The threshold crossing procedure yields estimates only 20% greater than the lower bound, but the bias is a function of the S/N and must be estimated. On the other hand, the maximum value, though it has a constant bias, has estimates that are 100% greater than those of the lower bound. Furthermore, the exponential weighting function essentially destroys the radar sidelobes. Because of these problems, the feedback integrator is limited in usefulness.

Two-pole Filter

The two-pole filter in Fig. 3(c) requires the storage of an intermediate calculation besides the integrated output and is described mathematically by

$$y_i = x_i - k_2 z_{i-1} \tag{10}$$

and

$$z_i = y_{i-1} + k_1 z_{i-1}, \tag{11}$$

where x_i is the input, y_i is the intermediate calculation, z_i is the output, and k_1 and k_2 are the two feedback values. The values [12,13] that maximize P_D are given by

$$k_1 = 2 \exp(-\zeta\omega_d/\sqrt{1-\zeta^2}) \cos(\omega_d \tau) \tag{12}$$

and

$$k_2 = \exp(-2\zeta\omega_d \tau/\sqrt{1-\zeta^2}), \tag{13}$$

where $\zeta = 0.63$, $N\omega_d\tau = 2.2$, and N is the number of pulses between the 3 dB points of the antenna. With this rather simple device, a weighting pattern similar to the antenna pattern can be obtained. The detection performance is within 0.15 dB of the optimal detector, and its angular estimates, as shown in Fig. 2, are about 20% greater than the Cramer-Rao lower bound. If the desired number of pulses integrated is changed because the rotation of the radar is changed or because another radar is used, it is necessary only to change the feedback values k_1 and k_2. The problems of this detector are that (a) it has rather high detector sidelobes, 15 to 20 dB and (b) it is extremely sensitive to interference (i.e., the filter has a high gain that results in a large output for a single sample that has a high value).

Binary Integrator

The binary integrator is also known as the dual-threshold detector, M-out-of-N detector, or rank detector (see section on Nonparametric Detectors). Numerous individuals have studied it [14-18]. As shown in Fig. 3(d), the input samples are quantized to 0 or 1 depending on whether or not they are less than a threshold T_1. The last N zeroes and ones are summed and compared to a second threshold $T_2 = M$. For large N, the detection performance of this detector is approximately 2 dB less than that of the moving-window integrator because of the hard limiting of the data, and the angular estimation error is about 25% greater than the Cramer-Rao lower bound. Schwartz [16] showed that within 0.2 dB, the optimal value of M for maximum P_D is given by

$$M = 1.5\sqrt{N} \tag{14}$$

when $10^{-10} < P_{fa} < 10^{-5}$ and $0.5 < P_D < 0.9$. Dillard [18], as shown in Fig. 8, calculated the optimal value of P_N, and the probability of exceeding T_1 when only noise is present. Then, the threshold T_1 is found from

$$P_N = \int_{T_1}^{\infty} \frac{x}{\sigma^2} e^{-x^2/2\sigma^2} dx, \tag{15}$$

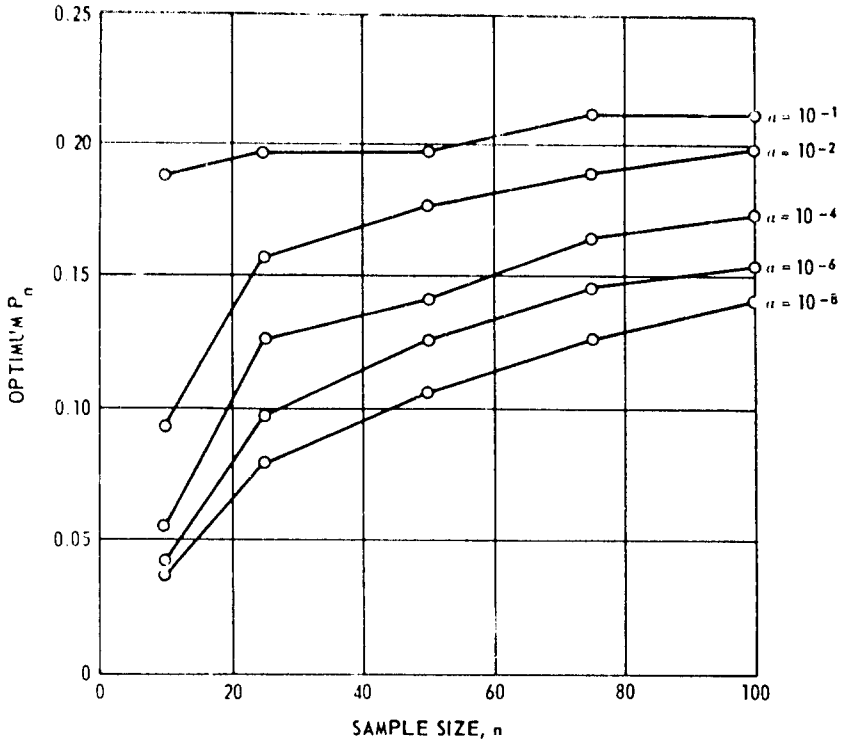

Fig. 8 — Optimum values of P_N as a function of the sample size, n; probability of false alarm, α; Rice distribution, $\theta = 1$, (copyright 1967, IEEE). From G.M. Dillard [18]

which yields

$$T_1 = \sigma\,(-2 \ln P_N)^{1/2}. \tag{16}$$

Figures 9 and 10 give a comparison of the optimal (best value of M) binary integrator with various other procedures.

The binary integrator is used in many radars because (a) it is easily implemented, (b) it ignores interference spikes that cause trouble with integrators directly using signal amplitude, and (c) it works extremely well when the noise has a non-Rayleigh density [19]. Figure 11 shows a comparison of the optimal binary integrator (three-out-of-three, M-out-of-N), another binary integration (two-out-of-three), and the moving window detector in log-normal interference (an example of a non-Rayleigh density). The optimal binary integrator is much better than the moving window integrator. The optimal values for log-normal interference were calculated by Schleher [19] and are $m = 3$, 8, and 25, for $n = 3$, 10, and 30 respectively.

A modified version of binary integration is used sometimes when there are a large number of pulses. It also has flexibility to integrate a different number of pulses. The modified binary moving window (MBMW) differs from the ordinary binary moving window (OBMW) because of the introduction of a third threshold. When the second threshold is reached, one counts the number of consecutive pulses for which the second threshold is exceeded. When this number equals the third threshold, a target is declared. The performance of the MBMW and a comparison to the OBMW are shown in Table 1 [20]. The larger the value of N, the larger is the difference in dB performance between the MBMW and OBMW detectors.

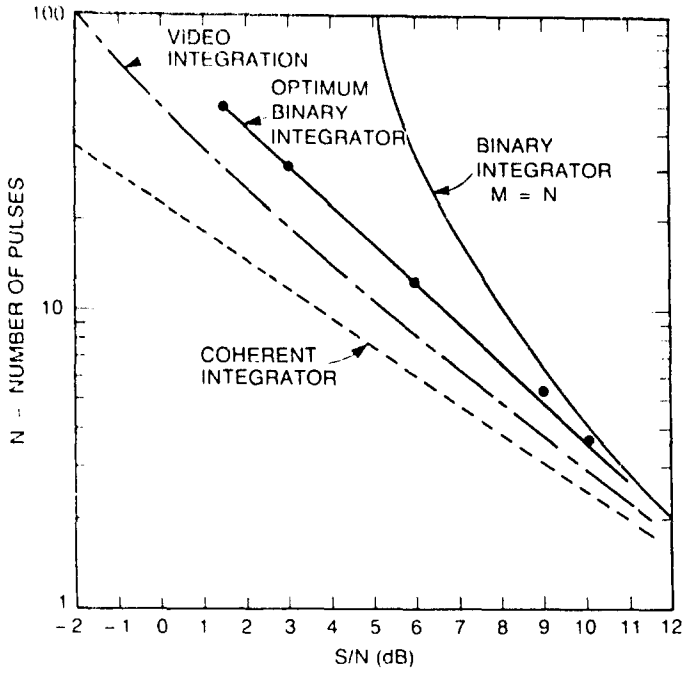

Fig. 9 — Comparison of binary integrators (M-out-of-N) with other integration methods ($P_{fa} = 10^{-10}$, $P_D = 0.5$), (copyright 1956, IEEE). From M. Schwartz [16]

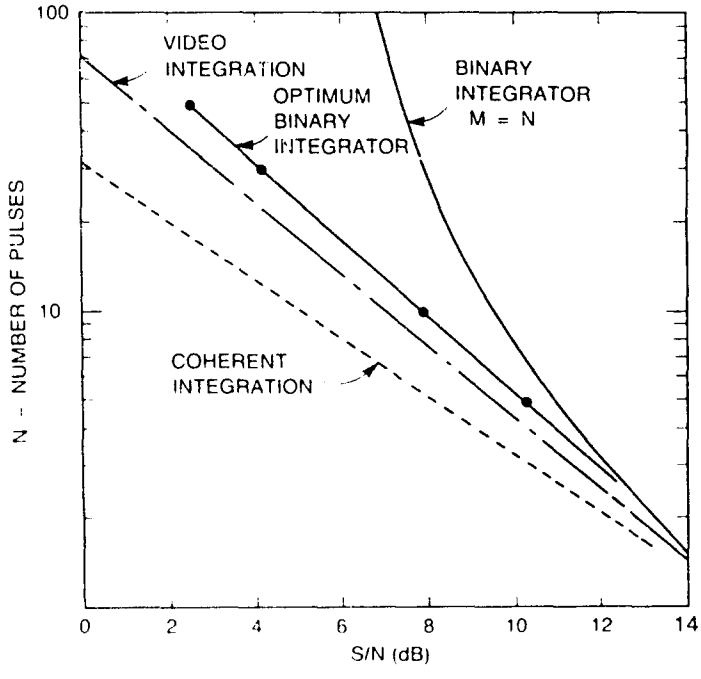

Fig. 10 — Comparison of binary integrator (M-out-of-N) with other integration methods ($P_{fa} = 10^{-10}$, $P_D = .90$). From M. Schwartz [16]

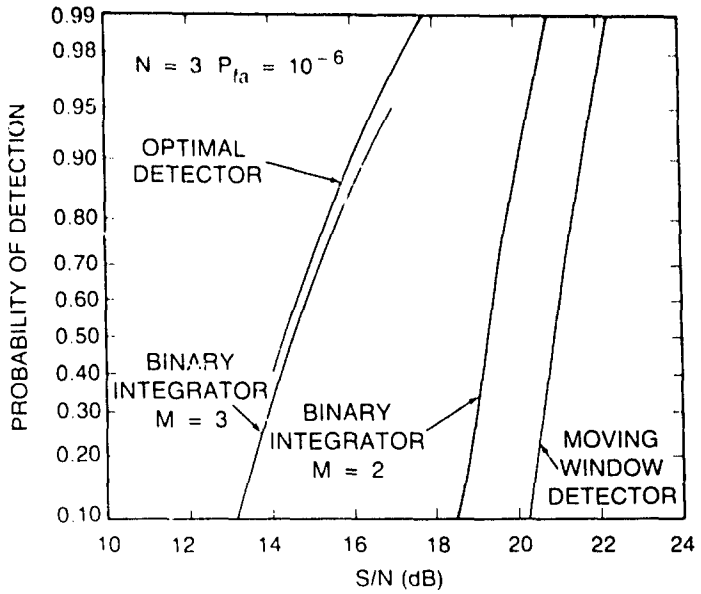

Fig. 11 — Comparison of various detectors in log-normal interference ($N = 3$, $P_{fa} = 10^{-6}$), (copyright 1975, IEEE). After D.C. Schleher [19]

Table 1 — Comparisons of the Detection Performance Between MBMW and OBMW at $N = 8, 16, 24, 32$ with $P_1 = 10^{-6}$, $P_D = 0.9$. After Mao [20]

Number of Pulses	Type of Detector	Detection Criteria	P_N	T_1	S/N(dB)
$N = 8$	MBMW	4/7 + 1	0.018	3.22	8.28
	OBMW	5/8	0.032	3.015	8.13
$N = 16$	MBMW	4/7 + 5	0.054	3.81	7.54
	MBMW	4, 3/7 + 7	0.060	2.77	7.01
	OBMW	8/16	0.064	2.74	6.21
$N = 24$	MBMW	4/7 + 6	0.071	2.70	7.34
	MBMW	4, 3/7 + 7	0.060	2.77	6.98
	OBMW	10/24	0.072	2.69	5.18
$N = 32$	MBMW	4/7 + 7	0.091	2.59	7.32
	MBMW	4, 3/7 + 7	0.060	2.77	6.98
	OBMW	13/32	0.095	2.57	4.53

Batch Processor

The batch processor is very useful when a large number of pulses are in the 3 dB beamwidth. If KN pulses are in the 3 dB beamwidth as shown in Fig. 3, K pulses are summed (batched) and either a 0 or 1 is declared depending on whether or not the batch is less than a threshold T_1. The last N zeros and ones are summed and compared to a second threshold M. An alternative version of this detector is to put the batches through a moving window detector.

The batch processor, like the binary integrator, is easily implemented, it ignores interference spikes, and works extremely well when the noise has a non-Rayleigh density. Furthermore, when compared with the binary integrator, the batch processor requires less storage, detects better, and estimates angles more accurately. For instance, if there were 80 pulses on target, one could batch 16 pulses, quantize this result to a 0 or 1, and declare a target with a 3-out-of-5 (or 2-out-of-5) binary integrator. With an 8 bit analog-to-digital converter, the storage requirement per range cell is 17 bits (12 bits for batch and 5 for binary integrator) for the batch processor as opposed to 80 bits for the binary integrator and 640 bits for the moving window. The detection performance of the batch processor for a large number of pulses integrated is approximately 0.5 dB worse than the moving window.

The batch processor has been successfully implemented by the Applied Physics Laboratory (APL) [21] of Johns Hopkins University. To obtain an accurate azimuth estimate approximately 20% greater than the lower bound, APL uses

$$\theta = \frac{\sum B_i \theta_i}{\sum B_i}, \tag{17}$$

where B_i is the batch amplitude and θ_1 is the azimuth angle that corresponds to the center of the batch.

False Alarm Control

In the presence of clutter, if fixed thresholds are used with the previously discussed integrators, an enormous number of detections will occur and will saturate and disrupt the tracking computer associated with the radar system. Four important facts should be noted:

- It makes little sense to have an automatic detection system without an associated tracking system;
- the P_{fa} of the detector should be as high as possible without saturating the tracking computer;
- Random false alarms and unwanted targets (e.g., stationary targets) are not a problem if they are removed by the tracking computer; and
- scan-to-scan processing is the only way to remove stationary point clutter or moving target indicator (MTI) clutter residues.

One can limit the number of false alarms with a fixed threshold system by setting a very high threshold. However, this would reduce target sensitivity in regions of low noise (clutter) return. To reduce the false-alarm problem, three main approaches have been used: adaptive threshold, nonparametric detectors, and clutter maps. Adaptive thresholding and nonparametric detectors assume that the samples in the range cells surrounding the test cell (called reference cells) are independent and identically distributed. Usually it is assumed that the time samples are independent. Both kinds of detectors test whether the test cell has a return sufficiently larger than the reference cells. Clutter maps allow variation in space but require stationarity over several scans. Clutter maps store an average background level for each range-azimuth cell. A target is then declared in a range-azimuth cell if the new value exceeds the average background level by a specified amount.

Adaptive Thresholding

The basic assumption of the adaptive thresholding technique is that the probability density of the noise is known except for a few unknown parameters. The surrounding reference cells are used to estimate the unknown parameters, and a threshold based on the estimated parameters is obtained. The simplest adaptive detector, shown in Fig. 12, is the cell-averaging CFAR investigated by Finn and Johnson [22]. If the noise has a Rayleigh density, $p(x) = x \exp(-x^2/2\sigma^2)/\sigma^2$, only the parameter σ needs to be estimated and the threshold is of the form $T = K\Sigma x_i = Kn\sqrt{\pi/2}\hat{\sigma}$. However, since T is set by an estimate $\hat{\sigma}$, it has some error and must be slightly larger than the threshold one would use if σ were known exactly a priori. The raised threshold causes a loss in target sensitivity and is referred to as a CFAR loss. This loss has been calculated [23] and is summarized in Table 2. Table 2 shows that for a small number of reference cells the loss is large because of the poor estimate of σ. Consequently, a large number of reference cells would be preferred. However, if this occurs, the homogeneity assumption (i.e., all the reference cells are statistically similar) might be violated. A good rule of thumb is to use enough reference cells so that the CFAR loss is below 1 dB and at the same time not let the reference cells extend beyond 1 mi on either side of the test cell. For a particular radar this might not be feasible.

If there is uncertainty about whether or not the noise is Rayleigh distributed, it is better to threshold individual pulses and use a binary integrator as shown in Fig. 13. This detector is tolerant to variations in the noise density because by setting K to yield a "1" with probability 0.1, a $P_{fa} \approx 10^{-6}$ can be obtained by using a 7-out-of-9 detector. Although noise may be non-Rayleigh, it will probably be very Rayleigh-like out to the tenth percentile. Furthermore, one can use feedback based on several scans of data to control K in order to maintain a desired P_{fa} either on a scan or sector basis, thus demonstrating the general rule that to maintain a low P_{fa} in various environments, adaptive thresholding should be placed in front of the integrator.

If the noise power varies from pulse-to-pulse (as it would in jamming when frequency agility is employed), one must CFAR each pulse and then integrate. While the binary integrator performs this type of CFAR action, analysis [24,25] has shown that the ratio detector shown in Fig. 14 is a better detector. The ratio detector sums S/N ratios and is specified by

$$\sum_{i=1}^{n} \frac{x_i^2(j)}{\frac{1}{2m}\sum_{k=1}^{m}[x_i^2(j+1+k) + x_i^2(j-1-k)]} \tag{18}$$

where $x_i(j)$ is the ith envelope-detected pulse in the jth range cell and the number of reference cells is 2 m. The denominator is the maximum likelihood estimate of σ_i^2, the noise power per pulse. It will detect targets even though only a few returned pulses have a high S/N ratio. Unfortunately, this will also cause the ratio detector to declare false alarms in the presence of narrow-pulse interference. To reduce the number of false alarms when narrow-pulse interference is present, the individual power ratios can be soft-limited [25] to a small enough value so that interference will only cause a few false alarms. Figures 15 and 16 show a comparison of the ratio detector with other commonly used detectors. Figure 17 shows a typical performance in sidelobe jamming when the jamming level varies by 20 dB per pulse. By employing a second test to identify the presence of narrow-pulse interference, a detection performance approximately halfway between the limiting and nonlimiting ratio detectors can be obtained.

If the noise samples are dependent in time or have a non-Rayleigh density, such as the chi-square density or log-normal density, it is necessary to estimate two parameters and the adaptive

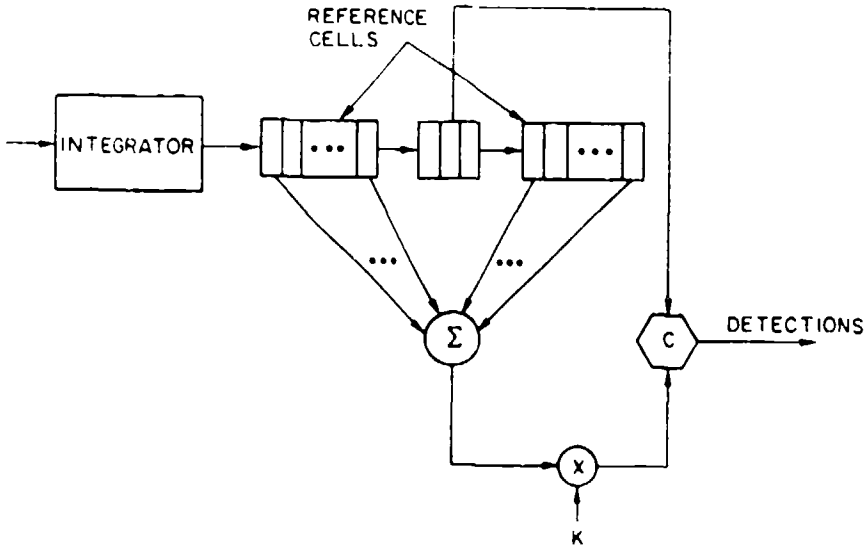

Fig. 12 — Cell-averaging. From CFAR [7]

Table 2 — CFAR Loss for $P_{fa} = 10^{-6}$ and $P_D = 0.9$.
After Mitchell and Walker [23]

Number of Pulses Integrated	Loss for Various Numbers of Reference Cells (dB)					
	1	2	3	5	10	∞
1	—	—	15.3	7.7	3.5	0
3	—	7.8	5.1	3.1	1.4	0
10	6.3	3.3	2.2	1.3	0.7	0
30	3.6	2.0	1.4	1.0	0.5	0
100	2.4	1.4	1.0	0.6	0.3	0

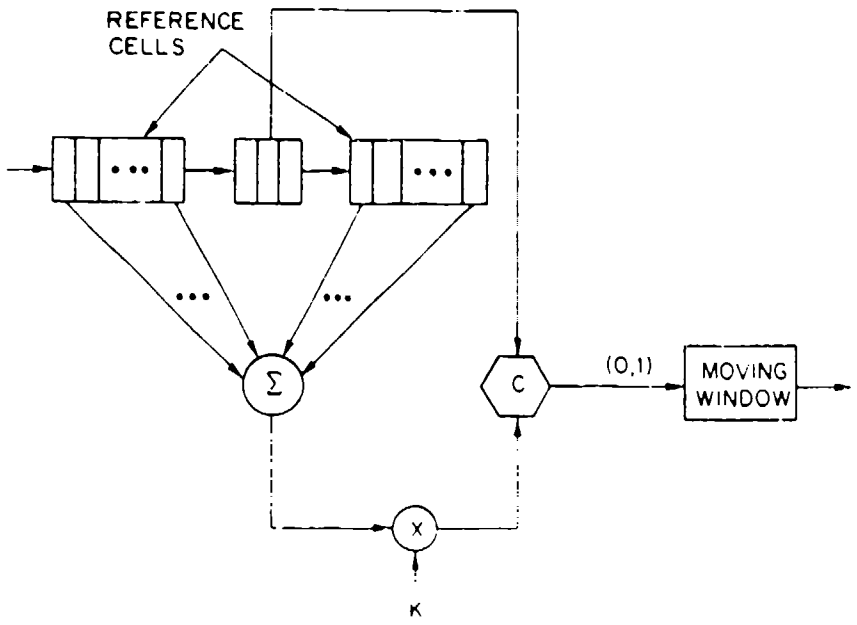

Fig. 13 — Implementation of binary integrator. From G.V. Trunk [7]

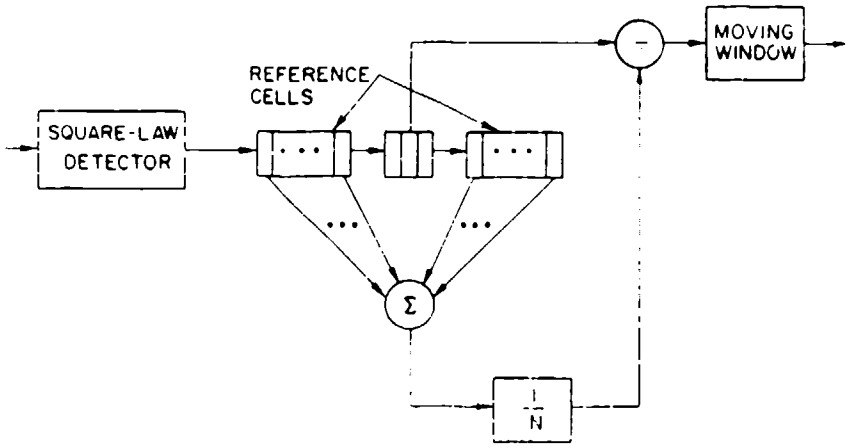

Fig. 14 — Ratio detector. From G.V. Trunk [7]

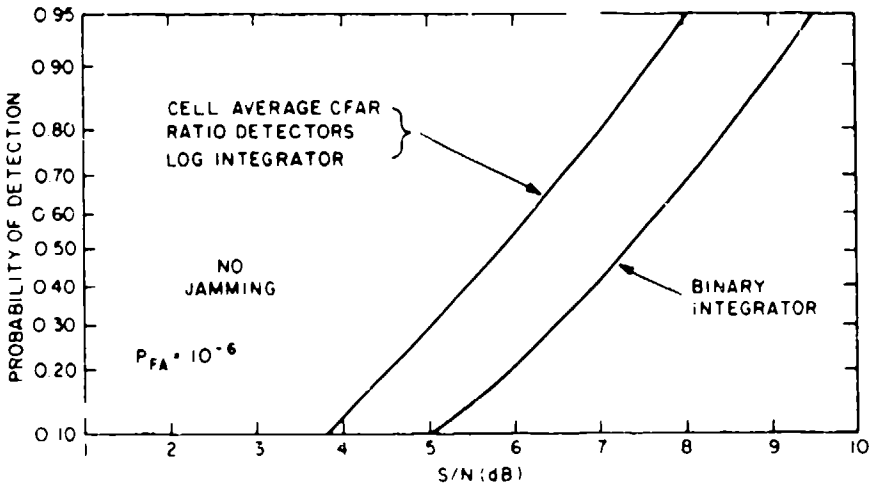

Fig. 15 — Curves of probability of detection vs signal-to-noise ratio per pulse for the cell-averaging CFAR, ratio detectors, log integrator, and binary integrator: nonfluctuating target and probability of false alarm = 10^{-6}. From G.V. Trunk [25]

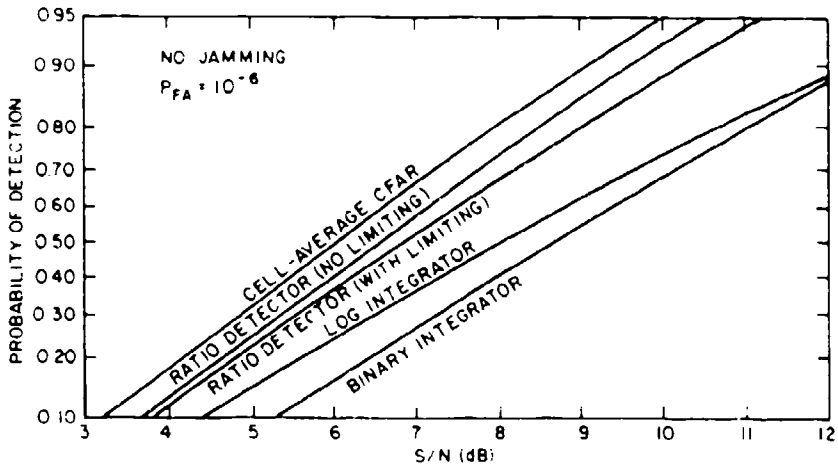

Fig. 16 — Curves of probability of detection vs signal-to-noise ratio for the cell-averaging CFAR, ratio detectors, log integrator, and binary integrator: Rayleigh fluctuating target and probability of false alarm = 10^{-6}. From G.V. Trunk [25]

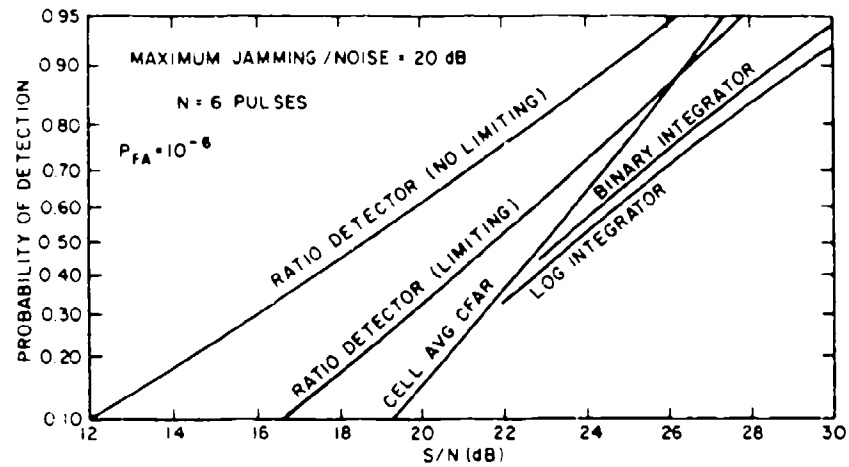

Fig. 17 — Curves of probability of detection vs signal-to-noise ratio for the cell-averaging CFAR, ratio detectors, log integrator, and binary integrator: Rayleigh fluctuations, probability of false alarm = 10^{-6} and maximum jamming-to-noise ratio = 20 dB. From G.V. Trunk [25]

detector is more complicated. Usually several pulses are integrated so that one can assume that the integrated output has a Gaussian probability density. Then the two parameters that must be estimated are the mean and variance, and a threshold of the form $T = \hat{\mu} + K\hat{\sigma}$ is used. Though the mean is easily obtained in hardware, the usual estimate of the standard deviation,

$$\hat{\sigma}^2 = \frac{1}{N} \sum (x_i - \bar{x})^2, \tag{19}$$

where

$$\bar{x} = \frac{1}{N} \sum x_i \tag{20}$$

is more difficult to implement. Consequently, the mean deviate defined by

$$\hat{\sigma} = A \sum |x_i - \bar{x}| \tag{21}$$

is sometimes used because it is easy to implement. Nothing can be done to the binary integrator to yield a low P_{fa} if the noise samples are correlated. Thus, it should not be used in this situation. However, if the correlation time is less than a batching interval, the batch processor will yield a low P_{fa} without modifications.

Target Suppression

Target suppression is the loss in detectability that is caused by other targets or clutter residues in the reference cells. Basically there are two approaches for solving this problem: (1) remove large returns from the calculation of the threshold [26,27]; (2) diminish the effects of large returns by either limiting or using log video. The technique that should be used is a function of the particular radar system and its environment.

Rickard and Dillard [27] proposed a class of detectors D_K where the K largest samples are censored from the reference cells. A comparison of D_0 (no censoring) with D_1 and D_2 for a Swerling 2 target is shown in Fig. 18, where N is the number of reference cells, β is the ratio of the power of the interfering target to the target in the test cell, and the bracketed pair (m,n) indicates the Swerling models of the target and the interfering target respectively. Figure 18 shows that when one has an interfering target the P_D does not approach 1 as S/N increases. Another approach [26], which censors samples in the reference cell if they exceed a threshold, is briefly discussed in the section about nonparametric detectors.

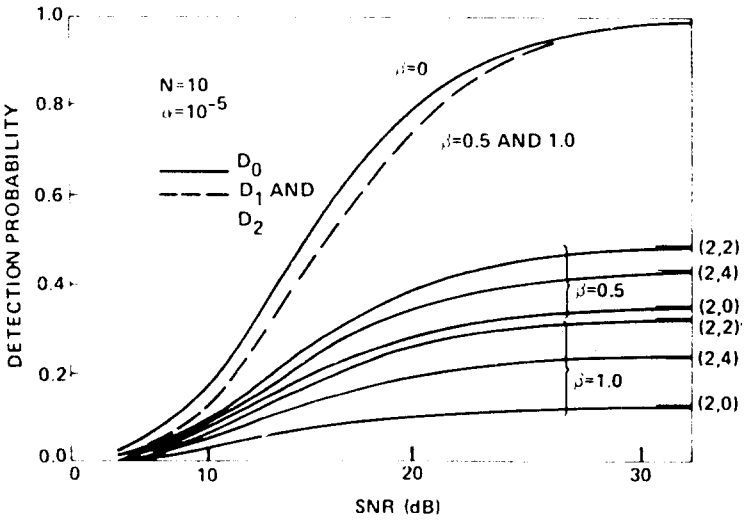

Fig. 18 — Detection probability vs SNR for Swerling case 2 primary target (copyright 1977, IEEE). From J.T. Rickard and G.M. Dillard [27]

The use of log video is an alternate approach for interfering targets. Basically by taking the log, large samples in the reference cells will have little effect on the threshold. The loss associated with the use of log video is 0.5 dB for 10 pulses integrated and 1.0 dB for 100 pulses integrated [28]. Figure 19 shows an implementation of the log-CFAR [29]. To maintain the same CFAR loss, the number of reference cell $M_{\log}$ for the log-CFAR should equal

$$M_{\log} = 1.65\, M_{lin} - 0.65, \tag{22}$$

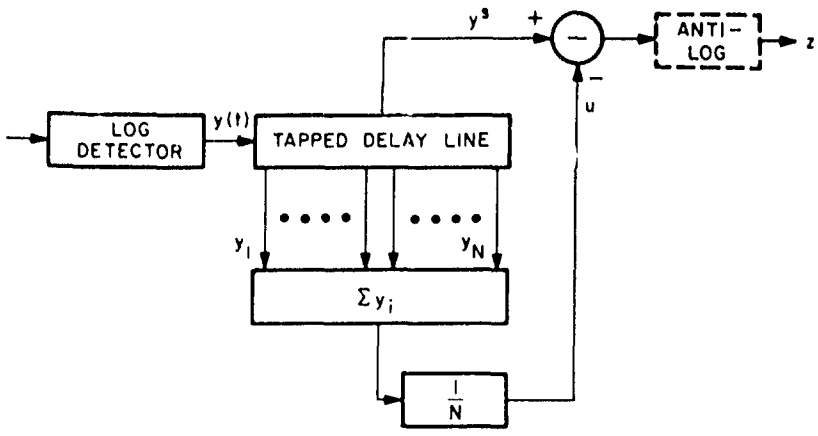

Fig. 19 — Block diagram of cell averaging LOG/CFAR receiver. (copyright 1972, IEEE). From V.G. Hansen and J.R. Ward [29]

where M_{lin} is the number of reference cells for linear video. The effect of target suppression with log video is discussed in the section on target resolution (Table 4).

Nonparametric Detectors

Nonparametric detectors obtain CFAR usually by ranking the test sample with the reference cells [30,31]. Specifically, one orders the samples from the smallest to the largest and replaces the smallest with the rank 0, the next smallest with rank 1, . . . , and the largest with rank $n - 1$. Under the hypothesis that all the samples are independent samples from an unknown density function, the test sample has equal probability of taking on any value. For instance, referring to the ranker in Fig. 20, the test cell is compared to 15 of its neighbors. Since in the set of 16 samples the test sample has equal probability of being the smallest sample (or equivalently any other rank), the probability that the test sample takes on values 0, 1, . . . , 15 is 1/16. A simple rank detector is constructed by comparing the rank to a threshold K, and then generating a 1 if the rank is equal or larger, a 0 if the rank is smaller. The 0s and 1s are summed in a moving window. This detector incurs a CFAR loss of about 2 dB but achieves a fixed P_{fa} for any unknown noise density as long as the time samples are independent. This detector was incorporated into a postprocessor used in conjunction with the Federal Aviation Administration's ASR radars. The major shortcoming of this detector is that it is fairly susceptible to target suppression (e.g., if a large target is in the reference cells, the test cell cannot receive the highest ranks).

If the time samples are correlated, the rank detector will not yield CFAR. A modified rank detector, called the modified generalized sign test (MGST) [26], maintains a low P_{fa} and is shown in Fig. 21. This detector can be divided into three parts: a ranker, an integrator (in this case a two-pole filter), and a threshold (decision process). A target is declared when the integrated output exceeds two thresholds. The first threshold is fixed (equals $\mu + T_1/K$, Fig. 19) and yields $P_{fa} = 10^{-6}$ when the reference cells are independent and identically distributed. The second threshold is adaptive and maintains a low P_{fa} when the reference samples are correlated. The device estimates the standard deviation of the correlated samples with the mean deviate estimator, where extraneous targets in the reference cells have been excluded from the estimate by use of a preliminary threshold T_2.

The rank and MGST detectors are basically two-sample detectors. They decide that a target is present if the ranks of the test cell are significantly greater than the ranks of the reference cells. Target suppression occurs at all interfaces (e.g., land, sea), where the homogeneity assumption is

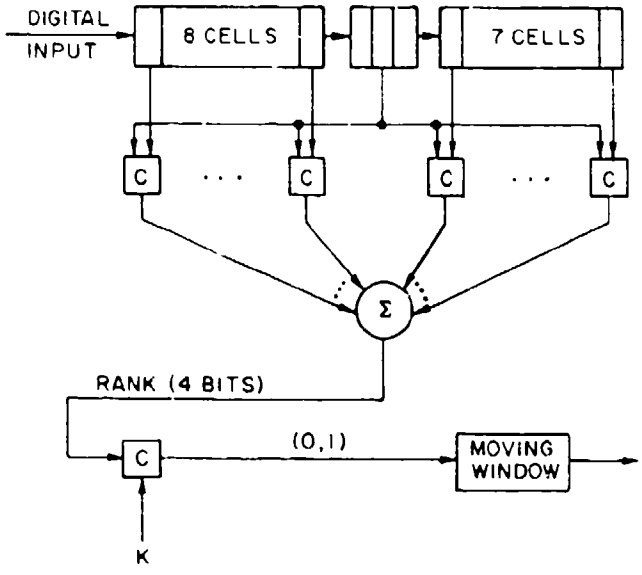

Fig. 20 — Rank detector: output of a comparator C is either a zero or one. From G.V. Trunk [7]

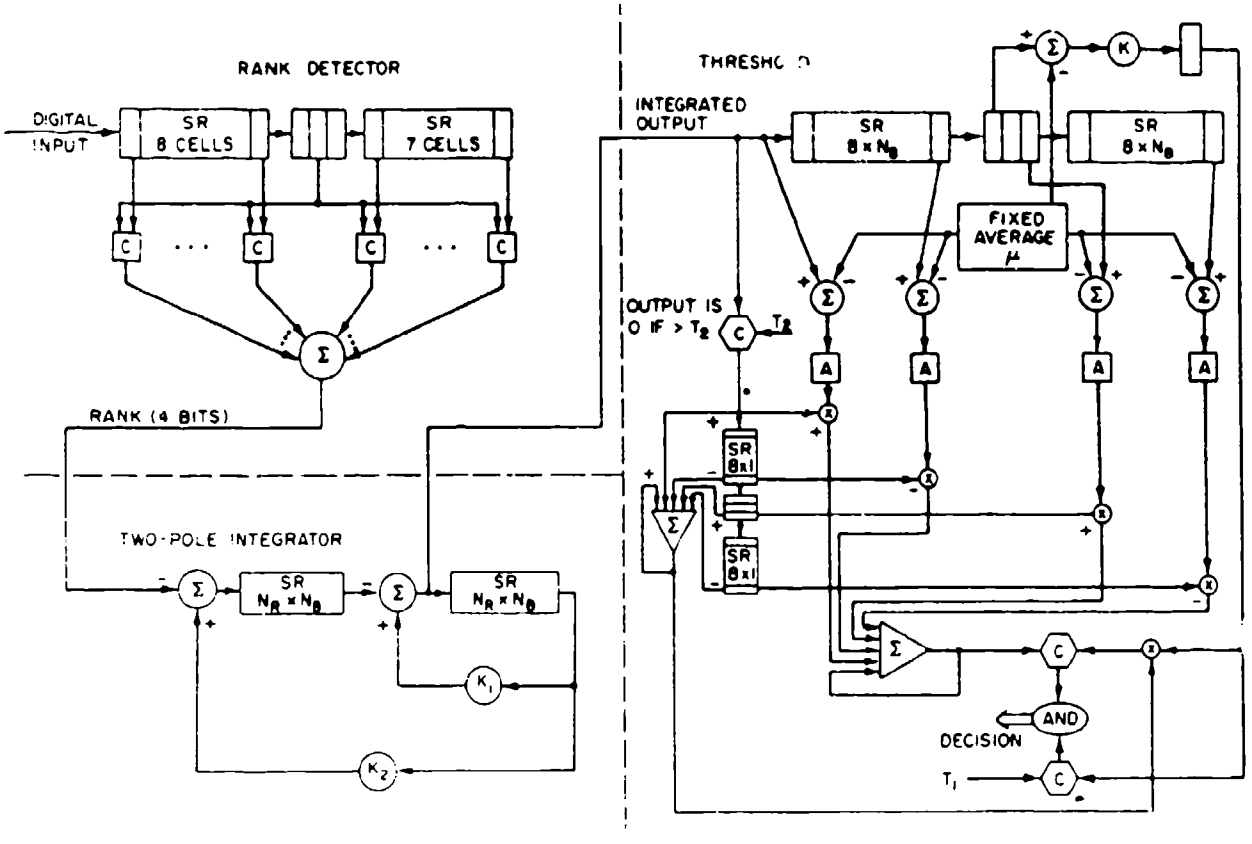

Fig. 21 — Modified generalized sign test processor, (copyright 1974, IEEE). From G.V. Trunk [26]

violated. However, some tests exist, such as Spearman Rho and Kendall Tau tests, that depend only on the test cell. These tests work on the principal that as the antenna beam sweeps over a point target, the signal return increases and then decreases. Thus, for the test cell, the ranks should follow the pattern of first increasing and then decreasing. Although these detectors do not require reference cells and hence have the useful property of not requiring homogeneity, they are not generally used because of the large CFAR loss taken for moderate sample sizes. For instance, the CFAR losses are approximately 10 dB for 16 pulses on target and 6 dB for 32 pulses on target [32].

A basic disadvantage of all nonparametric detectors is that one loses amplitude information, which can be a very important discriminant between target and clutter [33]. For example, a large return ($\sigma > 1000\text{m}^2$) in a clutter area is probably just clutter breakthrough. See "contact entry logic" in the section entitled Track-While-Scan System.

Clutter Mapping

A clutter map uses adaptive thresholding where the threshold is calculated from the return in the test cell on previous scans rather than from the surrounding reference cells on the same scan. This technique has the advantage that for essentially stationary environments (e.g., land-based radar against ground clutter), the radar has inter clutter visibility—it can see between large clutter returns. At the Lincoln Laboratory [34] they very effectively used a clutter map for the zero doppler filter in their Moving Target Detection (MTD). The decision threshold T for the ith pulse is

$$T = AS_{i-1} \tag{23}$$

where

$$S_i = K\, S_{i-1} + X_i\,, \tag{24}$$

S_i is the background level, X_i is the ith pulse, K is the feedback value that determines the map time constant, and A is the constant that determines the false alarm rate. In the MTD, used for ASR application, K is 7/8, which effectively averages the last eight scans. Several questions concerning the use of clutter maps remain unanswered: (1) if frequency agility is used, will there be a need to use a map for each frequency or can an average clutter map be used; (2) when there is slow moving clutter, such as rain and chaff, how should one update the map accounting for the clutter that moves from one cell to another; and (3) can clutter maps be used effectively on slowly moving platforms such as ships.

Target Resolution

In automatic detection systems, a single, large target will probably be detected many times; e.g., in adjacent range cells, azimuth beams, and elevation beams. Therefore, automatic detection systems have algorithms for merging the individual detections into a single centroided detection. However, most algorithms have been designed so that they will rarely ever split a single target into two targets, thus resulting in poor range resolution capability. A merging algorithm commonly used [35] is the adjacent-detection merging algorithm, which decides whether a new detection is adjacent to any of the previously determined set of adjacent detections. If the new detection is adjacent to any detection in the set of adjacent detections, it is added to the set. Two detections are adjacent if two of their three parameters (range, azimuth, and elevation) are the same and the other parameter differs by the resolution element: range cell ΔR, azimuth beamwidth θ, or elevation bandwidth γ. A simulation was run to compare the resolving capability of some common detection procedures shown in Fig. 22; and the

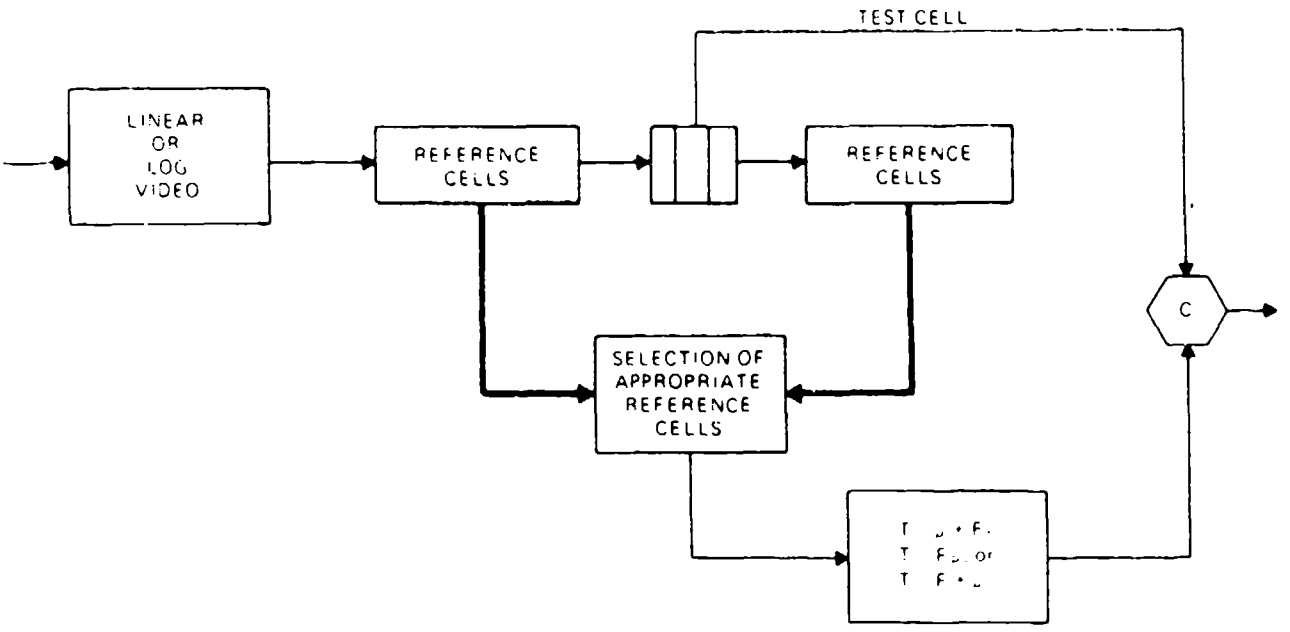

Fig. 22 — Variations of basic detector. T is the threshold, μ is either the mean of all the reference cells or is the smaller (the minimum) of the means of the reference cells at only the right and of the reference cells at only the left, F is a fixed number, and σ is the variance, (copyright 1978, IEEE). From G.V. Trunk [35]

results are shown in Table 3. As demonstrated, the log detectors have much better performance than the detectors using linear video. The effect of target suppression on log video can be seen in Table 4. One notes an improved performance when one calculates the threshold using only the half of the reference with the minimum mean value. Figure 23 shows the resolution capability of the log detector that uses only the reference cells with the minimum mean. The probability of resolving two equal amplitude targets does not rise above 0.9 until they are separated in range by 2.5 pulsewidths.

Assuming that the target is small with respect to the pulsewidth and that the pulse shape is known, the resolution capability can be improved by fitting the pulse shape to the data and comparing the residue square error to a threshold [36]. If only one target is present, the residue should only be noise and hence should be small. If two or more targets are present, the residue will contain signal and should be large. The results of resolving two targets with S/N = 20 dB are shown in Fig. 24. These targets can be resolved at a resolution probability of 0.9 at separations that vary between 1/4 and 3/4 of a pulsewidth depending on the relative phase difference between the two targets. Furthermore, this result can be improved further by processing multiple pulses.

Detection Summary

When only 2 to 4 samples (pulses) are available, a binary integrator should be used to avoid detections from interference. When a moderate number of pulses (5 to 16) are available, a binary integrator, rank detector, or moving window integrator should be used. If the number pulses is large (greater than 20), a batch processor or two-pole filter should be used. If the samples are independent, a one parameter threshold can be used. If the samples are dependent, one can either use a two parameter threshold or adapt a one-parameter threshold on a sector basis. These rules should only serve as a general guideline. It is *highly recommended* that the radar video from the environment of interest be collected and analyzed and that various detection processes be simulated on a computer and tested against recorded data.

Table 3 — Number of Targets Detected when Two Targets are Separated by 1.5, 2.0, 2.5, 3.0, or 3.5 Range-Cells and the Third Target is 7.0 Cells from the First Target. From Trunk [35]

Number of Times the Two Closely Spaced Targets Were Detected Out of 50 Opportunities										
Target Separation (ΔR)	Linear Detector $T = \mu + F\sigma$			Linear Detector $T = F\mu$			Log Detector $T = F + \mu$			
	Zero Targets	One Target	Two Targets	Zero Targets	One Target	Two Targets	Zero Targets	One Target	Two Targets	Three Targets
Threshold based on all reference cells										
1.5	46	4	0	2	43	5	0	48	2	0
2.0	49	1	0	14	13	23	0	23	27	0
2.5	50	0	0	10	32	8	0	3	46	1
3.0	49	1	0	0	10	20	0	6	44	0
Threshold based on minimum of reference cells										
1.5	0	49	1	0	49	1	0	50	0	0
2.0	0	47	3	0	31	19	0	28	22	0
2.5	0	48	2	0	12	38	0	1	49	0
3.0	0	49	1	0	18	32	0	1	49	0

Table 4 -- Number of Targets Detected when Two Targets are Separated by 1.5, 2.0, 2.5, or 3.0 Range-Cells. S/N of Target 1 = 20 dB.
SNR of Target 2 = 10, 13, 20, 30, or 40 dB. From Trunk [35]

Number of Times a Given Number of Targets Were Detected Out of 50 Opportunities										
Target Separation (ΔR)	SNR = 10 dB		SNR = 13 dB		SNR = 20 dB		SNR = 30 dB		SNR = 40 dB	
	One Target	Two Targets	One Target	Two Targets	One Target	Two Targets	One Target	Two Targets	One Target	Two Targets
Threshold based on all reference cells										
1.5	50	0	48	2	48	2	50	0	50	0
2.0	50	0	39	11	23	27	43	7	45	5
2.5	48	2	38	12	3	47	19	31	34	16
3.0	50	0	38	12	6	44	4	46	11	39
Threshold based on minimum of reference cells										
1.5	50	0	49	1	50	0	50	0	49	1
2.0	45	5	34	16	28	22	44	6	48	2
2.5	41	9	21	29	1	49	27	23	36	14
3.0	39	11	17	33	1	49	9	41	13	37

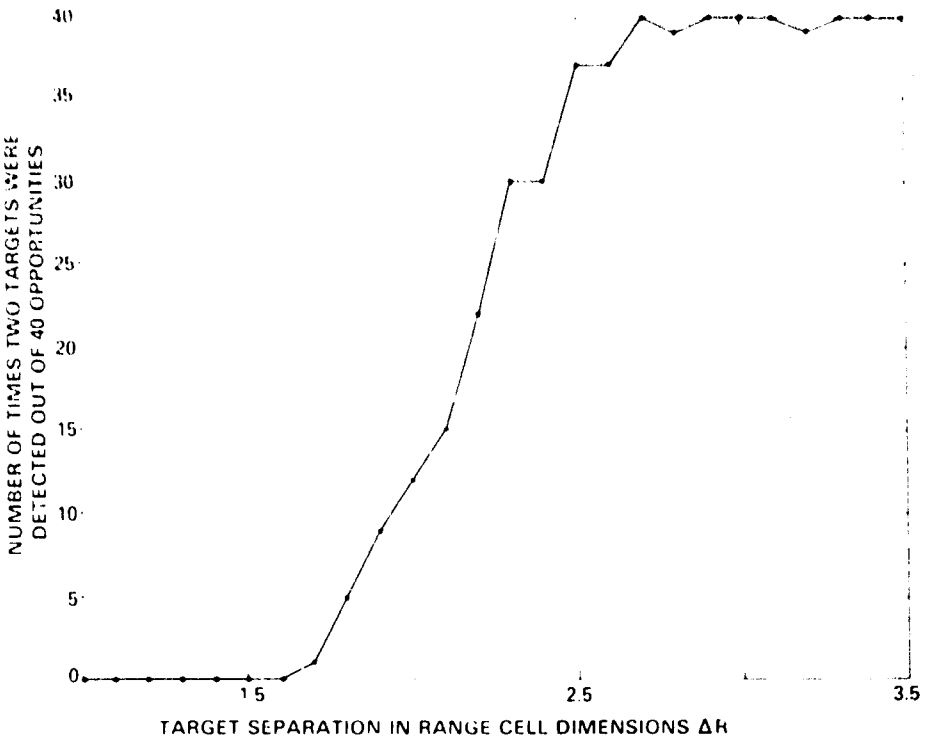

Fig. 23 — Resolution capability of log detector that uses reference cells with minimum mean. (copyright 1978, IEEE). From G.V. Trunk [35]

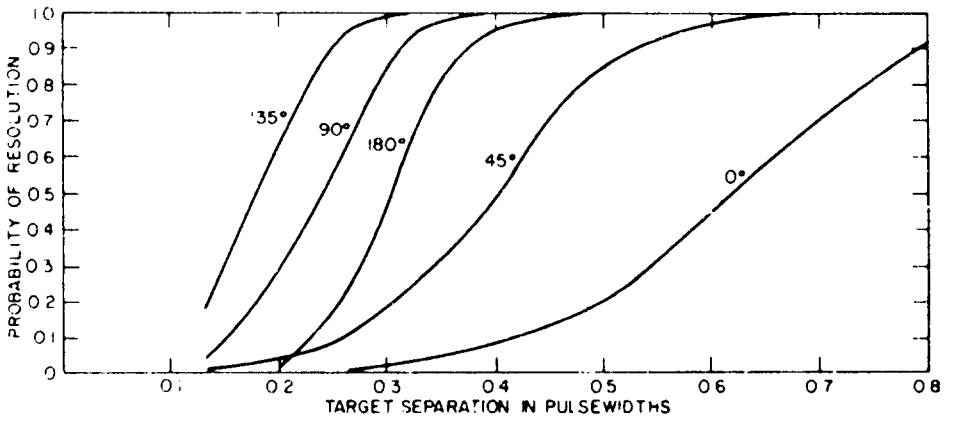

Fig. 24 — Probability of resolution as a function of range separation: coherent ad hoc procedure; sampling rate $\Delta R = 1.5$ samples per pulsewidth; target strengths—nonfluctuating, $A_1 = A_2 = 20$ dB; phase differences = 0°, 45°, 90°, 135°, and 180°, (copyright 1984, IEEE). From G.V. Trunk [36]

AUTOMATIC TRACKING

Track-while-scan systems are tracking systems for surveillance radars whose nominal scan time (revisit time) is from 4 to 12 s. If the probability of detection (P_D) per scan is high, if accurate target location measurements are made, if the target density is low, and if there are only a few false alarms, the design of the correlation logic and tracking filter is straightforward. However in a realistic radar environment these assumptions are seldom valid, and the design of the automatic tracking system is complicated. In actual situations one encounters target fades (changes in signal strength caused by multipath propagation, blind speeds, and atmospheric conditions), false alarms (caused by noise, clutter, interference, and jamming), and poor radar parameter estimates (caused by noise, unstabilized antennas, unresolved targets, target splits, multipath propagation, and propagation effects). The tracking system must deal with all these problems.

A generic track-while-scan will be considered first. This will be followed by a discussion of maximum likelihood, multiple scan approaches to automatic tracking.

Track-While-Scan System

A general outline of a track-while-scan system is presented. Next, since a major portion of any tracking system must deal with manipulating a large amount of data efficiently, a typical file system and pointer system are described. Then the contact entry logic, coordinate systems, tracking filter, maneuver-following logic, track initiation, and correlation logic are discussed in detail.

System Organization

Almost all track-while-scan systems operate on an azimuthal sector basis that provides basic system timing. Figure 25 shows a typical series of operations. For instance, if the radar has reported all the detections in sector 11 and is now in sector 12, the tracking program would start by correlating (trying to associate) the clutter points (stationary tracks) in sector 10 with detections in sectors 9, 10, 11. Those detections that are associated with clutter points are deleted (are not used for further correlations) from the detection file and are used to update the clutter points. Next, firm tracks in sector 8 are correlated with detections in sectors 7, 8, and 9. By this time all clutter points have been removed from sectors 9 and below. Those detections that are associated with firm tracks are deleted from the detection file and are used to update the appropriate track.

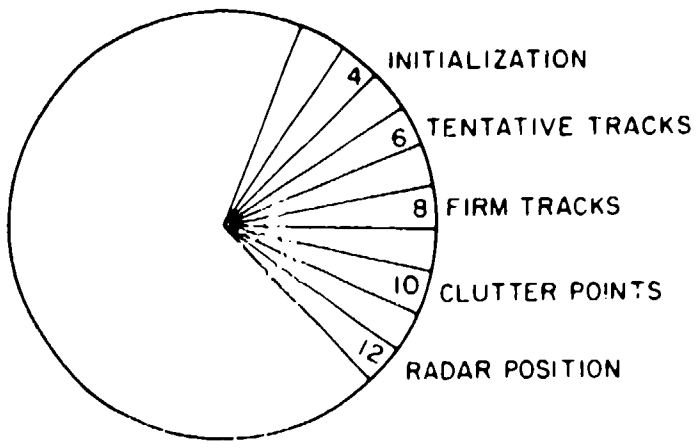

Fig. 25 – Various operations of a track-while-scan system performed on a sector basis. From G.V. Trunk [7]

Usually, some provision is made for giving preference to firm tracks (instead of tentative tracks) in the correlation process. By performing the correlation process two sectors behind firm-track correlations (Fig. 25), it is impossible for tentative tracks to steal detections belonging to firm tracks. In some other tracking systems the correlation for firm and tentative tracks is performed in the same sector; however, the generalized distance D (see Eq. (49)) between tracks and detections is incremented by ΔD if the track is tentative.

Finally, detections that are not associated with either clutter points or tracks are used for initiation of new tracks. The most common initiation procedure is to initiate a tentative track. Later the tentative track is dropped or else made a firm track or clutter point depending on its velocity. An alternate approach [37] is to establish both a clutter point and a tentative track. If the detection came from a stationary target, the clutter point will be updated and the tentative track will eventually be dropped. However, if the detection came from a moving target, the tentative track will be made firm and the clutter point will be dropped. This method requires less computer computation time when most of the detections are clutter residues.

File System

When a track is established in the software of the computer, a track number is assigned to it. All parameters associated with a given track are referred to by this track number. Typical track parameters are smoothed and predicted position and velocity, time of last update, track quality, covariances matrices if a Kalman type filter that is being used, and track history (i.e., the last n detections). Each track number is also assigned to a sector so that the correlation process can be performed efficiently [38]. In addition to the track file, a clutter file is maintained. A clutter number is assigned to each stationary or very slowly moving target. All parameters associated with a clutter point are referred to by this clutter number. Again, each clutter number is assigned to a sector in azimuth for efficient correlation.

The basic files and pointer systems are described below in a FORTRAN format. Note that several higher level languages such as PASCAL have pointer systems that permit efficient implementation.

Track and Clutter Number Files—Only the operation of the track number file is described, since the operation of clutter number file is identical. The development in Ref. 38 is used. The track number parameters are listed in Table 5.

Table 5 — Track Number Parameters. From Cantrell et al. [38]

Parameters	Description
NT	Track number
DROPT	1 (obtain) or 0 (drop) a track number NT
FULLT	Number of available track numbers
NEXTT	Next track number available
LASTT	Last track number not being used
LISTT(M)	File whose M locations correspond to track numbers
M	Maximum number of tracks

The track number file is initialized by setting LISTT(I) = I + 1 for I = 1 through M. LISTT(M) is set equal to zero (denoting the last available track number in the file), NEXTT = 1 (the next available track number), LASTT = M (the last track number not being used), and FULLT = M − 1 (indication that M − 1 track numbers are available). Figure 26 shows a flowchart of the operation.

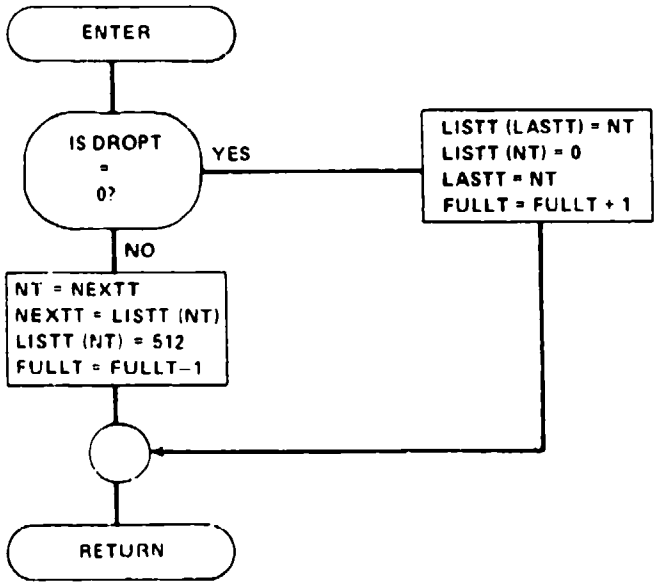

Fig. 26 — Flowchart for track number file. From B.H. Cantrell, G.V. Trunk, and J.D. Wilson [38]

When a new track number is requested, DROPT is set equal to one, and the system checks to see if FULLT is zero. If FULLT is not equal to zero the routine is called. Since DROPT = 1, the new track is assigned the next available track number; i.e., NT = NEXTT. The next available track number in the list is found, and NEXTT is set equal to LISTT(NT). FULLT is decremented, thus indicating that one less track number is available. Finally, LISTT(NT) is set equal to 512 (a number larger than the number of possible tracks). This is not necessary but sometimes helps in debugging the program.

When DROPT = 0, a track number NT is dropped by setting the last available track number LISTT(LASTT) equal to the track number NT. LISTT(NT) is set equal to zero to denote the last track number, and LASTT is then set equal to the track number being dropped, LASTT = NT. The parameter FULLT is incremented, indicating that one more track number is available. Thus, the track (and clutter) number files maintain a linkage from one number to the next, thereby eliminating searching techniques.

Track Number Assignment to Azimuth Sector Files—The azimuth-range plane is usually separated into 64 or 128 equal azimuth sectors. After a track is updated or initiated, the predicted position of the target is checked to see which sector it occupies, and the track is assigned to this sector. If the track is dropped or moves to a new sector, it is dropped out of the sector in which it was previously located. The parameters associated with the track sector files are listed in Table 6. Only the assignment of track numbers to azimuth sectors is described, since the clutter number assignment is identical. The TBX(I) file contains the first track number in sector I. If TBX(I) = 0, no tracks are in sector I. The IDT(M) file has storage locations corresponding to each of the possible M track numbers.

Table 6 -- Track Sector Files. From Cantrell et al. [38]

Parameter	Description
TBX(I)	First track number in sector I (a subscript of array IDT)
IDT(M)	Each location corresponds to a track number, and the location contains the next track number in sector I or a zero.

The first track number in sector I is obtained from FIRST = TBX(I). The second track number in the sector is obtained by NEXT1 = IDT(FIRST). The next track number in the sector is obtained by NEXT2 = IDT(NEXT1). The process is continued until a zero is encountered, indicating that no more track numbers are in the sector.

When a new track is added or a track moves from one sector to another, a track number must be added to the new sector. The flowchart for achieving this is shown in Fig. 27. The first track number in the sector is stored, the track number NT being added is made the first track number in the sector, and the track number NT in the IDT(NT) file is made equal to the original first track in the sector. This procedure is essentially a push-down stack that pushes the older track numbers further down in the file.

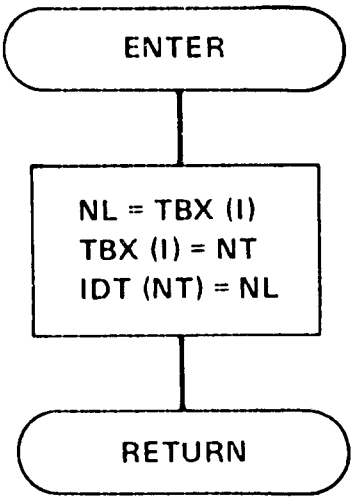

Fig. 27 -- Adding a track number NT to sector I. From B.H. Cantrell, G.V. Trunk, and J.D. Wilson [38]

When a track is dropped or moves out of the sector, the track number must be removed from the sector. Figure 28 shows the flow diagram for this. First, it is determined whether the first track number in the sector TBX(I) is the one being dropped. If it is, the first track number in the sector is set equal to the second track number in the sector, and the location in the IDT file corresponding to the track number NT being dropped is set to zero. NT is set equal to the track number in the file following the one just dropped, so that we now have the next available track number. If the track number being dropped is not the first one in the file, then the push-down stack IDT(NL) is searched sequentially until the track number is found. The variable IDT(NL) containing NT as the next track is replaced by the next track number following NT, and the variable in the IDT file corresponding to NT is set equal to zero. Again, NT is set equal to the track number in the file after the one being dropped.

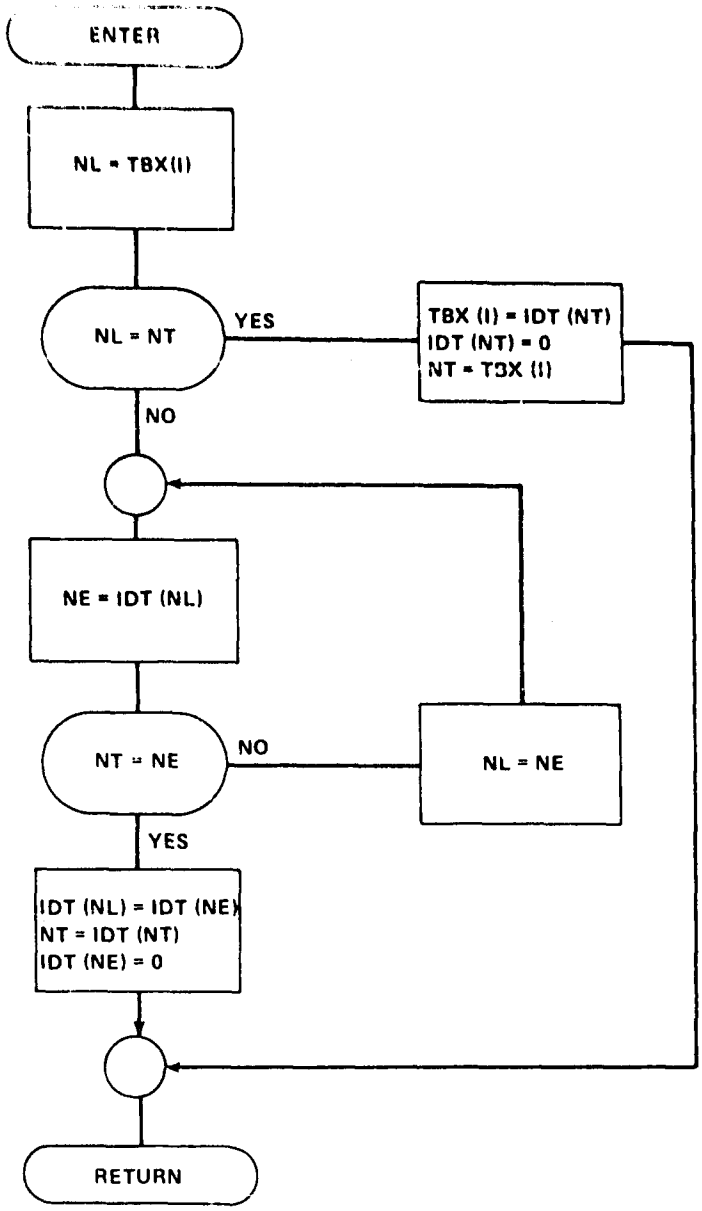

Fig. 28 — Dropping a track number NR from sector I. From B.H. Cantrell, G.V. Trunk, and J.D. Wilson [38]

Contact Entry Logic

Not all the detections declared by the automatic detector are used in the tracking process; rather, many of the detections (contacts) are filtered out in software using a process called "contact entry logic" [33]. The basic idea is to use the target amplitude in connection with the type of environment the detection comes from to eliminate some detections. The first step is for the operator to identify the environment in various regions. Types of environments that can be identified are land clutter, rain clutter, sea clutter, and interference. Histograms of detections in various regions are developed and Fig. 29 shows an example for rain clutter. In general, the amplitude of rain clutter detections is lower than that of targets. Consequently a threshold can be set to inhibit low-amplitude detections. This threshold can be controlled by the local detection density: raised in high-detection densities and lowered in low-detection densities. In no circumstances would a detection be inhibited if it fell within

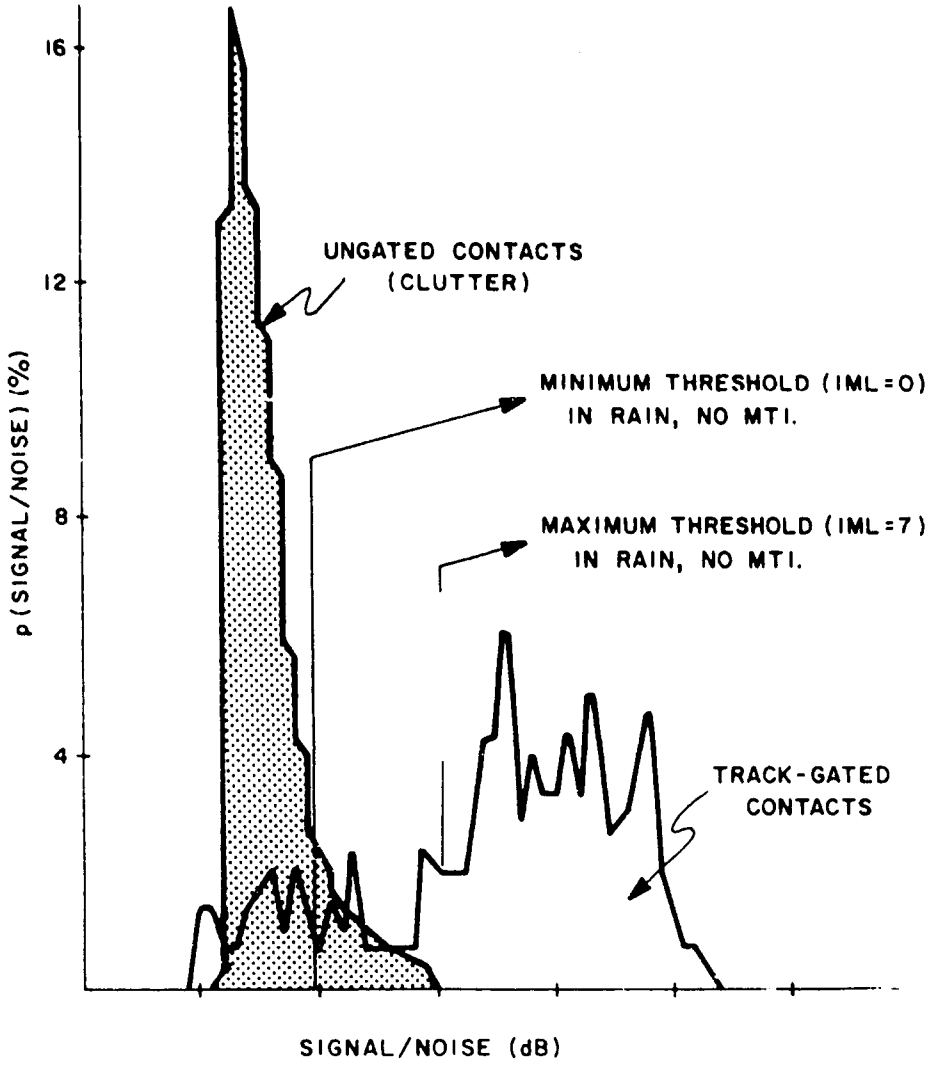

Fig. 29 — Effectiveness of signal/noise ratio test in rain clutter. From
From W.G. Bath, L.A. Biddson, S.F. Haase, and E.C. Wetzlar [33]

a track-gate (i.e., gate centered about the predicted position of a firm track). In land clutter areas, high-amplitude detections would be inhibited.

Coordinate Systems

The target location measured by the radar is in spherical coordinates: range, azimuth, elevation, and possibly range rate (doppler). Thus, it may seem natural to perform tracking in spherical coordinates. However, this causes difficulties since the motion of the constant-velocity targets (straight lines) will cause acceleration terms in all coordinates. A simple solution to this problem is to track in a Cartesian coordinate system. Although it may appear that tracking in Cartesian coordinates will seriously degrade the accurate range track, it has been shown [39] that the inherent accuracy is maintained. Another approach [40] noted that since maneuvering targets cause a large range error but a rather insignificant azimuth error, a target-oriented Cartesian coordinate system could be used. Specifically, the x axis is taken along the azimuth direction of the target and the y axis is taken in the cross-range direction. Finally, no matter what coordinate system is used for tracking, the correlation of detections with tracks must be performed in spherical coordinates.

Tracking Filters

The simplest tracking filter is the α-β filter described by

$$x_s(k) = x_p(k) + \alpha[x_m(k) - x_p(k)], \tag{25}$$

$$V_s(k) = V_s(k - 1) + \beta[x_m(k) - x_p(k)]/T, \tag{26}$$

$$x_p(k + 1) = x_s(k) + V_s(k)\,T, \tag{27}$$

where $x_s(k)$ is the smoothed position, $V_s(k)$ is the smoothed velocity, $x_p(k)$ is the predicted position, $x_m(k)$ is the measured position, T is the scanning period (time between detections), and α and β are the system gains.

The minimal mean-square error (MSE) filter for performing the tracking when the equation of motion is known is the Kalman filter, first discussed by Kalman [41] and later by Kalman and Bucy [42]. The Kalman filter is the most commonly used filter in radar and is a recursive filter that minimizes the MSE. The state equation in xy coordinates for a constant-velocity target is

$$X(t + 1) = \Phi(t)\,X(t) + \Gamma(t)\,A(t), \tag{28}$$

where

$$X(t) = \begin{bmatrix} x(t) \\ \dot{x}(t) \\ y(t) \\ \dot{y}(t) \end{bmatrix}, \quad \Phi(t) = \begin{bmatrix} 1 & T & 0 & 0 \\ 0 & 1 & 0 & 0 \\ 0 & 0 & 1 & T \\ 0 & 0 & 0 & 1 \end{bmatrix} \tag{29}$$

$$\Gamma(t) = \begin{bmatrix} T^2/2 & 0 \\ T & 0 \\ 0 & T^2/2 \\ 0 & T \end{bmatrix}, \text{ and } A(t) = \begin{bmatrix} a_x(t) \\ \\ a_y(t) \end{bmatrix} \tag{30}$$

with $X(t)$ being the state vector at time t consisting of position and velocity components $\dot{x}(t)$, $x(t)$, $\dot{y}(t)$ and $y(t)$; $t + 1$ being the next observation time; T being the time between observations; and $a_x(t)$ and $a_y(t)$ being random accelerations with covariance matrix $Q(t)$. The observation equation is

$$Y(t) = M(t)\,X(t) + V(t), \tag{31}$$

where

$$Y(t) = \begin{bmatrix} x_m(t) \\ y_m(t) \end{bmatrix}, \quad M(t) = \begin{bmatrix} 1 & 0 & 0 & 0 \\ 0 & 0 & 1 & 0 \end{bmatrix}, \text{ and } V(t) = \begin{bmatrix} v_x(t) \\ v_y(t) \end{bmatrix}, \tag{32}$$

with $Y(t)$ being the measurement at time t consisting of positions $x_m(t)$ and $y_m(t)$ and $V(t)$ being a zero-mean noise whose covariance matrix is $R(t)$.

The problem is solved recursively by first assuming the problem is solved at time $t - 1$. Specifically, it is assumed that the best estimate $\hat{X}(t-1|t-1)$ at time $t-1$ and its error covariance matrix $P(t-1|t-1)$ are known, where the caret in the expression of the form $\hat{X}(t|s)$ signifies an estimate and the overall expression signifies $X(t)$ is being estimated with observations up to $Y(s)$. The six steps involved in the recursive algorithm are:

- calculate the one-step prediction

$$\hat{X}(t|t-1) = \Phi(t-1)\,\hat{X}(t-1|t-1); \tag{33}$$

- calculate the covariance matrix for the one-step prediction

$$P(t|t-1) = \Phi(t-1)\,P(t-1|t-1)\Phi^T(t-1) + \Gamma(t-1)Q(t-1)\Gamma^T(t-1); \tag{34}$$

- calculate the predicted observation

$$\hat{Y}(t|t-1) = M(t)\hat{X}(t|t-1); \tag{35}$$

- calculate the filter gain

$$\Delta(t) = P(t|t-1)\,M^T(t)\,[M(t)P(t|t-1)M^T(t) + R(t)]^{-1}; \tag{36}$$

- calculate the new smoothed estimate

$$\hat{X}(t|t) = \hat{X}(t|t-1) + \Delta(t)\,[Y(t) - \hat{Y}(t|t-1)]; \text{ and} \tag{37}$$

- calculate the new covariance matrix

$$P(t|t) = [I - \Delta(t)M(t)]\,P(t|t-1). \tag{38}$$

In summary, starting with an estimate $\hat{X}(t-1)(t-1)$ and its covariance matrix $P(t-1|t-1)$ after a new observation $Y(t)$ is received and the six quantities in the recursive algorithm are calculated, a new estimate $\hat{X}(t|t)$ and its covariance matrix $P(t|t)$ are obtained.

It can be shown [43] that for a zero random acceleration, $Q(t) \equiv 0$ and a constant measurement covariance matrix $R(t) = R$, the α-β filter can be made equivalent to the Kalman filter by setting

$$\alpha = \frac{2(2k-1)}{k(k+1)} \tag{39}$$

and

$$\beta = \frac{6}{k(k+1)} \tag{40}$$

on the kth scan.

Thus with time, α and β approach zero, and heavy smoothing is applied to the new samples. Usually it is worthwhile to bound α and β from zero by assuming a random acceleration $Q(t) \neq 0$

corresponding to approximately a 1-g maneuver. The previously stated Kalman filter method is optimal (with respect to MSE) for straight-line tracks but must be modified to enable the filter to follow target maneuvers.

Maneuver-Following Logic

Benedict and Bordner [44] noted that in track-while-scan systems, there is a conflicting requirement between good tracking noise reduction (implying small α and β) and good maneuver-following capability (implying large α and β). Although some compromise is always required, the smoothing equations should be constructed to give the best compromise for a desired tracking noise reduction. Benedict and Bordner defined a measure of transient-following capability and showed that α and β should be related by

$$\beta = \frac{\alpha^2}{2 - \alpha}. \tag{41}$$

Thus, an (α, β) pair satisfying Eq. (41) can be chosen so that the tracking filter will follow a specified g-turn. Cantrell [45] calculated the probability that a target detection will fall within a correlation region centered at the predicted target position when the target is doing a specified g-turn. He suggested using the (α,β) pair satisfying Eq. (41) that yields the smallest correlation region. However, if high g-turns must be followed, the noise performance is poor.

An alternate approach uses a turn detector (Fig. 30) that consists of two correlation regions. The inner nonmaneuvering gate is usually set so that the probability of the target detection being in the gate is greater than 0.99 when the target is doing a 1-g maneuver. Then, if the detection is in the nonmaneuvering correlation region, the filter operates as usual, the filter gains being reduced according to Eq. (36) or Eqs. (39) and (40). When the target detection falls outside the inner gate but within the maneuver gate, a maneuver is declared and the filter bandwidth is increased (α and β are increased)—Quigley and Holmes [46] increase the bandwidth by lowering the value of k in Eqs. (39) and (40). To avoid the problem of a target fading causing a missed detection and a false alarm appearing in the large maneuver gate, the track should be bifurcated when a maneuver is declared. That is, two tracks are generated: the continuation of the old track but not updated with the new detection and a new maneuvering track with the new detection and increased filter bandwidth. The next scan is used to resolve the ambiguity and remove one of the tracks. Although the turn detector is the most common approach for maneuver-following, other solutions are to adjust the bandwidth as a function of the measurement error [37] or to use the Kalman filter with a realistic target-maneuvering model [47].

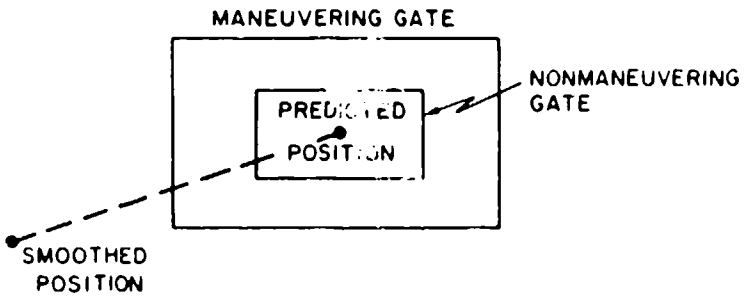

Fig. 30 -- Maneuver and nonmaneuver gates centered at the target's predicted position. From G.V. Trunk [7]

Specifically, Cantrell et al. [37] suggested that the α-β filter (described by Eqs. (25) through (27)) be made adaptive by adjusting α and β by

$$\alpha = 1 - e^{-2\zeta\omega_0 T} \tag{42}$$

and

$$\beta = 1 + e^{-2\zeta\omega_0 T} - 2e^{-\zeta\omega_0 T} \cos(\omega_0 T\sqrt{1-\zeta^2}), \tag{43}$$

in which

$$\omega_0 = 0.5\,|p_1(k)/p_2(k)|\,, \tag{44}$$

where

$$p_1(k) = e^{-\omega_a T} p_1(k-1) + (1 - e^{-\omega_b T})\,\epsilon(k)\,\epsilon(k-1)\,, \tag{45}$$

$$p_2(k) = e^{-\omega_b T} p_2(k-1) + (1 - e^{-\omega_b T})\,\epsilon(k)\epsilon(k)\,, \tag{46}$$

ζ is the damping coefficient (nominally 0.7), T is the time since the last update, ω_a and ω_b are weighting constants, and $\epsilon(k)$ is the error between the measured and predicted positions on the kth update. The basic principle of the filter is that $p_1(k)$ is an estimate of the covariance of successive errors and $p_2(k)$ is an estimate of the error variance. When the target trajectory is a straight line, $p_1(k)$ approaches 0, since the expected value of $\epsilon(k)$ is 0. Thus ω_0 approaches 0, and the filter performs heavy smoothing. When the target turns, $p_1(k)$ grows, since the error $\epsilon(k)$ will have a bias. Thus ω_0 grows, and the filter can follow the target maneuver.

Singer [47] suggested using the Kalman filter with a realistic target-maneuvering model. He assumed that the target was moving at a constant velocity but was perturbed by a random acceleration. The target acceleration is correlated in time; and it was assumed that the covariance of the correlation was

$$r(\tau) = E\{a(t)\,a(t+\tau)\} = \sigma_m^2\, e^{-\gamma|\tau|}\,, \tag{47}$$

where $a(t)$ is the target acceleration at time t, σ_m^2 is the variance of the target acceleration, and γ is the reciprocal of the maneuver time constant. The density function for target acceleration consists of delta functions at $\pm A_{\max}$, a delta function at 0 with probability P_0, and a uniform density between $-A_{\max}$ and $A_{\max}$. For this density

$$\sigma_m^2 = \frac{A_{\max}^2}{3}\,(1 + 4P_{\max} - P_0). \tag{48}$$

For this target motion, Singer then calculated the state transition matrix $\phi(t)$ and the covariance matrix $Q(t)$, thereby specifying the Kalman-filter solution. He generated curves that give the steady-state performance of the filter for various data rates, single-look measurement accuracies, encounter geometry, and class of maneuvering targets.

Track Initiation

Detections that do not correlate with clutter points or tracks are used to initiate new tracks. If the detection does not contain doppler information, the new detection is usually used as the predicted position (in some military systems, one assumes a radially inbound velocity); and a large correlation region must be used for the next observation. The correlation region must be large enough to capture the next detection of the target that has the maximum velocity of interest. Since the probability of obtaining false alarms in the large collection region is sometimes large, one should generally disregard the initial detection if no correlation is obtained on the second scan. Also one should not declare a track firm until at least a third detection (falling within a smaller correlation region) is obtained. A common track initiation criteria is four out of five, although one may require only three detections out of five in regions with low false alarm and target density rates. The possible exceptions for using only two detections are when doppler information is available (so that a small correlation region can be used immediately and the range rate can be used as an additional correlation parameter) or for "pop-up" targets (i.e., targets that suddenly appear at a close range) in a military situation.

An alternative track initiation logic [40] uses a sequential hypothesis-testing scheme. When a correlation is made on the ith scan, Δ_i is added to a score function; when a correlation opportunity is missed, Δ_i' is subtracted from the score function. The increments are a function of the state of the tracking system, the closeness of the association, the number of false alarms in the region, the a priori probability of targets, and the probability of detection. When the score function exceeds a particular value, the track becomes firm. Although this method will inhibit false tracks in dense detection environments, it will not necessarily establish the correct tracks.

To initiate tracks in a dense detection environment, the technique known as "retrospective processing" [48] uses the detections over the last several scans to initiate straight-line tracks by using a collection of filters matched to different velocities. Figure 31 illustrates an example of the processing; here one looks for surface targets in the presence of sea spikes. It is clear from this figure that detections 1, 4, 6, 10, 12, and 14 form a track. Even though the false alarm rate per scan is relatively high (approximately 10^{-3}), the processor can be implemented with a microprocessor.

Track Drop

Firm tracks that are not updated in several scans corresponding to 40 to 60 s usually are dropped. In some systems, before a track is dropped the track symbol is blinked thus indicating a track is about to be dropped. This gives an operator the chance to update the track with a detection and keep it from being dropped.

Correlation Logic

Several procedures are used to associate detections with tracks. Of special interest are the conflicting situations of multiple tracks competing for a single detection or of multiple detections lying within a track's correlation gate.

To limit the number of detections that can update a track, correlation gates are used. A detection never will update a track unless it lies within the correlation gate that is centered at the track's predicted position. The correlation gate should be defined in $r - \theta$ coordinates, regardless of what coordinate system is used for tracking. Furthermore, the gate's size should be a function of the measurement accuracy and prediction error (specified by Eq. (34)) so that the probability of the correct detection lying within the gate is high (at least 0.99). In some tracking systems [49], the location of the correlation gate is fed back to the automatic detector; and the detection threshold is lowered in the

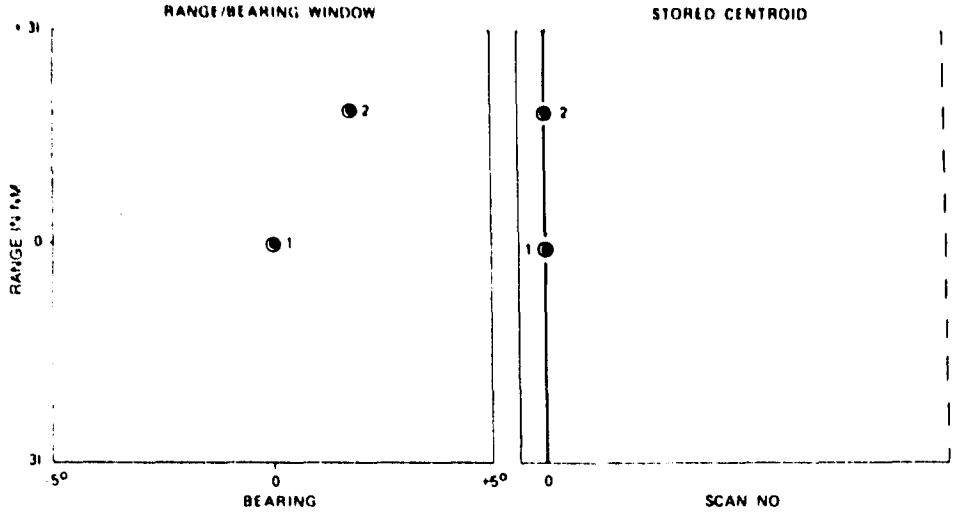

Fig. 31(a) -- The retrospective process: a single scan of data.
From R.J. Prengman, R.E. Thurder, and W.B. Bath [8]

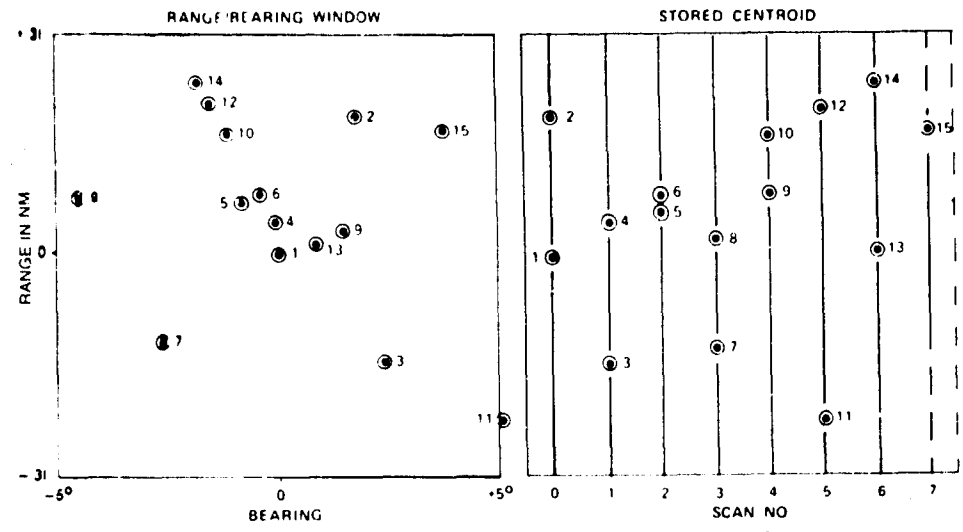

Fig. 31(b) — The retrospective process: eight scans of data.
From R.J. Prengman, R.E. Thurder, and W.B. Bath [48]

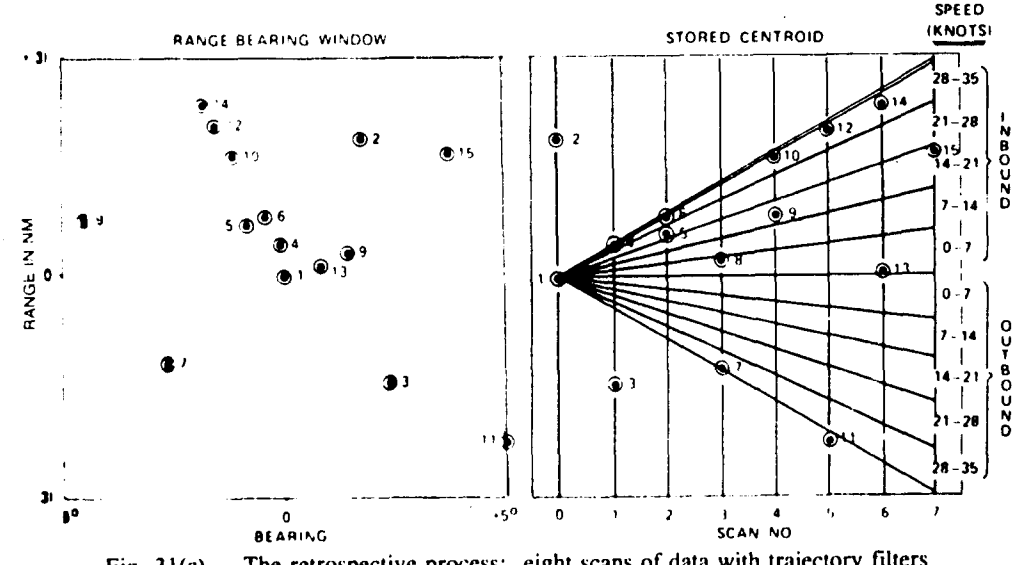

Fig. 31(c) — The retrospective process: eight scans of data with trajectory filters applied. From R.J. Prengman, R.E. Thurder, and W.B. Bath [48]

gate to increase the probability of detection P_D. The gate also disables the "contact entry" logic described in this section.

When several detections are within the correlation regions, the usual and simplest solution is to associate the closest detection with the track. Specifically, the measure of closeness is the statistical distance

$$D^2 = \frac{(r_p - r_m)^2}{\sigma_r^2} + \frac{(\theta_p - \theta_m)^2}{\sigma_\theta^2} \tag{49}$$

where (r_p, θ_p) is the predicted position, (r_m, θ_m) is the measured position, σ_r^2 is the variance of $r_p - r_m$, and σ_θ^2 is the variance of $\theta_p - \theta_m$. These variances are a by-product of the Kalman filter. Since the prediction variance is proportional to the measurement variance, σ_θ^2 and θ_r^2 are sometimes replaced by the measurement variances. Statistical distance rather than Euclidean distance must be used because the range accuracy is usually much better than the azimuth accuracy.

Figure 32 illustrates problems associated with multiple detections and tracks; two detections are within gate 1, three detections are within gate 2, and one detection is within gate 3. Table 7 lists all detections within the tracking gate, and the detections are entered in the order of their statistical distance from the track. Tentatively, the closest detection is associated with each track, and then the tentative associations are examined to remove detections that are used more than once. Detection 8, which is associated with tracks 1 and 2, is paired with the closest track (track 1 in this case); then all other tracks are reexamined to eliminate all associations with detection 8. Detection 7 is associated with tracks 2 and 3; the conflict is resolved by pairing detection 7 with track 2. When the other association with detection 7 is eliminated, track 3 has no associations with it and consequently will not be updated on this scan. Thus track 1 is updated by detection 8, track 2 is updated by detection 7, and track 3 is not updated.

An alternate strategy is to always pair a detection with a track if there is only one correlation with a track. As before, ambiguities are removed by using the smallest statistical distance. Thus, track 3 in the example is updated by detection 7, track 1 is updated by detection 8, and track 2 is updated by detection 9. This procedure yields better results when P_D is close to one and the probability of false alarm is very low.

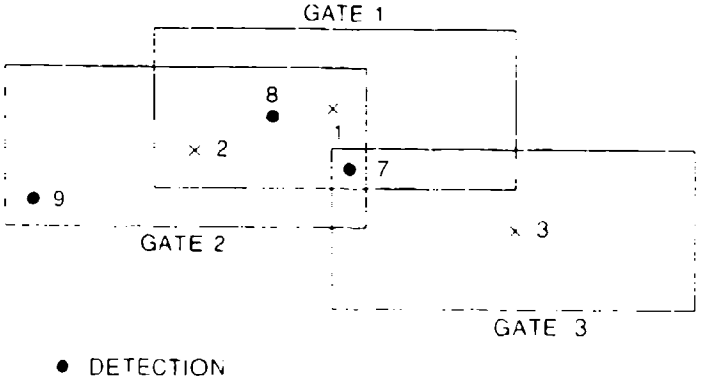

Fig. 32 — Examples of the problems caused by multiple detections and tracks in close vicinity. From G.V. Trunk [7]

Table 7 — Association Table for the Example Shown in Fig. 32. From Trunk [7].

Track Number	Closest Association		Second Association		Third Association	
	Detection Number	D^2	Detection Number	D^2	Detection Number	D^2
1	8	1.2	7	4.2	—	—
2	8	3.1	7	5.4	9	7.2
3	7	6.3	—	—	—	—

The optimal strategy that maximizes the probability of correct correlation is a joint maximum likelihood approach. This involves examining all possible combinations and selecting the combination that is most probable in a statistical sense. This procedure requires knowing the probability of detection and probability of false alarms. A discussion of the joint maximum likelihood approach can be found in the section entitled Maximum Likelihood Approaches.

Singer and Sea [50] were two of the first people to recognize and characterize the interaction between the correlation and track update functions. Specifically, three distinct situations can occur: the track is not updated, the track is updated with the correct return, and the track is updated with an incorrect return. They generalized the tracking filter's error covariance equations to account for the a priori probability of incorrect returns being correlated with the track. This permits the analytical evaluation of tracking accuracy in a multitarget environment that produces false correlations. Furthermore, by using the generalized tracking error covariance equation, they optimized the filter gain matrix that yielded a new minimum-error tracking filter for multitarget environments. Also, they generated a suboptimal fixed-memory version of this filter to reduce computation and memory requirements.

A subsequent paper by Singer et al. [51] uses a posteriori correlation statistics based on all reports in the vicinity of the track. The mathematical structure is similar to that of the Kalman filter. The estimation error is denoted by $\tilde{X}(t \mid t') = \hat{X}(t) - X(t \mid t')$ and has mean and covariance matrices denoted by $b(t \mid t')$ and $P(t \mid t')$. It is assumed that n_k detections fall within the correlation gate on scan k. Included in the number n_k are extraneous reports whose number obeys a Poisson distribution and whose positions are uniformly distributed within the gate. The smooth estimate is given by

$$\hat{X}(t \mid t) = \hat{X}(t \mid t - 1) + A(t), \tag{50}$$

where $A(t)$ is chosen to minimize the noncentral second moment of the filter estimation error.

The problem is solved by using track histories. A track history α at scan k is defined by selecting, for each scan, a detection or a miss (a miss corresponds to the hypothesis that none of the reports belong to the track). The number of such track histories is

$$L(k) = \sum_{i=1}^{k} (1 + n_i). \tag{51}$$

Associated with each history α is the probability $p_\alpha(t)$ that the history α is the correct one, given observations through time t (scan k). The terms $b'_\alpha(t \mid t - 1)$ and $P'_\alpha(t \mid t - 1)$ are the bias and

covariance of the estimation error $\tilde{X}(t \mid t-1)$, given observations through time $t-1$ and given that track history α' at time $t-1$ is the (only) correct one. Recursive equations are obtained for p_α, b_α, and P_α; then as shown, the optimal correction vector is given by

$$A(t) = \sum_{\alpha=1}^{L(k)} p_\alpha(t) b_\alpha(t \mid t-1). \tag{52}$$

This solution not only minimizes the mean-square error but also is an unbiased estimate.

The optimal a posteriori filter requires a growing memory; therefore several suboptimal filters were investigated by Singer et al. [51]. The first suboptimal filter considers only the last N scans; track histories that are identical for the last N scans are merged. The second suboptimal filter only considers the L nearest neighbors in the correlation gate; essentially the gate size is changed to limit the number of reports to L. The last method uses both techniques: it considers only the last N scans and restricts the number of reports on any scan to L.

Figures 33 and 34 show the results of simulations that compare the optimal and suboptimal a posteriori filters, the optimal and suboptimal a priori filters, and the Kalman filter. In Fig. 33, the filter variance normalized by the theoretical (perfect-correlation) Kalman-filter variance is plotted for several filters. As a class the a posteriori filters provide better performance than the other filters. However, for high density of false reports ($4\beta\sigma_R^2 = 0.1$), the a posteriori filter is 30 times worse than predicted by the standard Kalman-filter approach. Thus the standard approach should never be used in dense-target (or false-target) environments. Figure 34 gives the probability of making a false correlation. Again the a posteriori filters provide the best performance.

If one considers only the last scan ($N = 0$ case), one obtains the probabilistic data association filter (PDAF) [52,53]. In essence, each detection is used to update a Kalman filter and the final estimate is the weighted sum of all the estimates of each detection where the weight is the probability that each detection is the proper update. This procedure does not require a growing memory; it requires slightly higher computational requirements than the ordinary Kalman filter and solves the correlation problem by using all detections with the track gate to update the filter. As originally formulated, track initiation and termination were not considered. However, Colegrove et al. [54,55] have proposed solutions to these problems. Furthermore, they have implemented the PDAF on an OTH radar.

Maximum Likelihood Approaches

The previously discussed procedures updated a single track with either zero, one, or multiple detections; however, each track was operated on individually; i.e., each track was considered by itself. Better performance can be obtained by using all the detections, on all the previous scans by employing a maximum likelihood approach. This better performance is obtained at the cost of an enormous computational requirement.

Sittler [56] formulated the maximum likelihood approach to tracking. In his approach he assumed that: (a) objects appeared in the surveillance region according to a Poisson model and were uniformly distributed in space, (b) the persistence of objects is independent with a duration that follows an exponential density, (c) the track positions have a known density, (d) the detection model is a Poisson process, (e) the measurement errors have a known density (later assumed to be Gaussian), and (f) the false alarms follow a Poisson process.

Stein and Blackman's [57] approach is similar to that of Sittler [56]. It differs in the following ways: (a) a sample data system is assumed and the detection process is specified by the detection

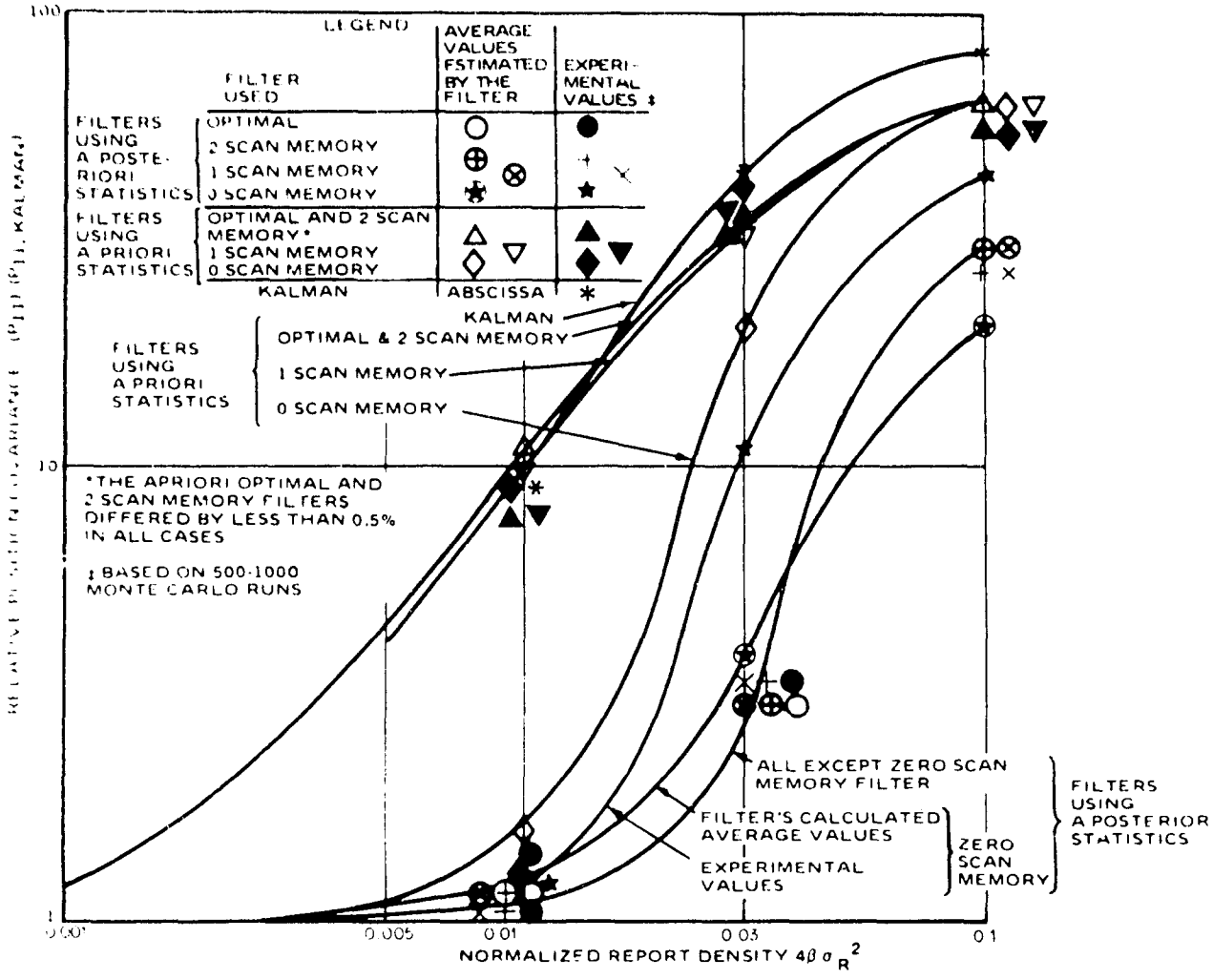

Fig. 33 — Simulated and calculated variances in filtered position errors for optimal and suboptimal a posteriori and a priori tracking filters, (copyright 1974, IEEE). From R.A. Singer, R.G. Sea, and K.B. Housewright [51]

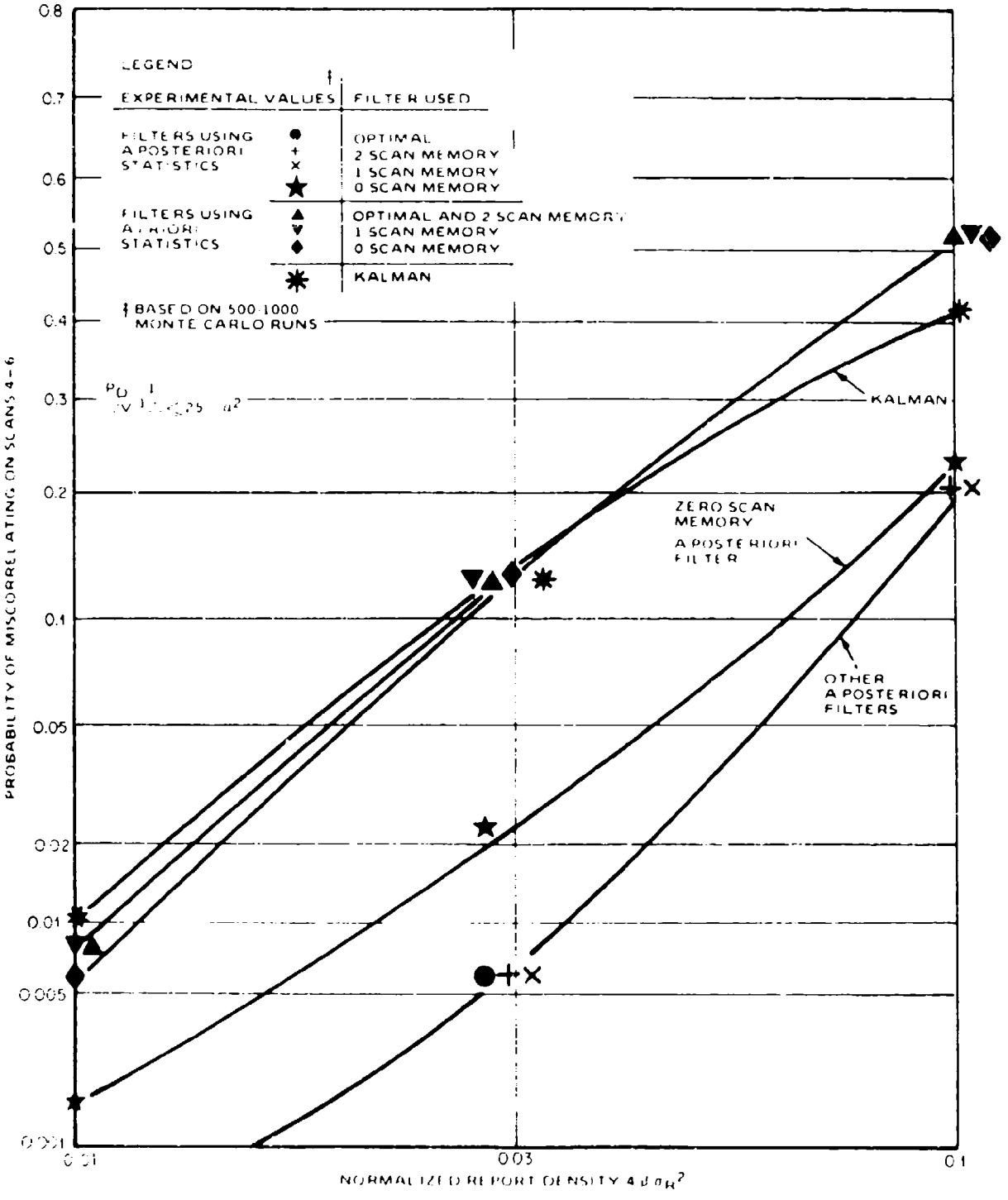

Fig. 34 Simulated probability of divergence or lost track for optimal and suboptimal a posteriori and a priori tracking filters. (Copyright 1974, IEEE). From R.A. Singer, R.G. Sea, and K.B. Housewright [51]

probability, (b) the development eliminates the concept of undetected targets and of distinguishing between true targets generating a single detection and false alarms, (c) it uses realistic target maneuver models [45], and (d) it uses the Kalman filter [41,42]. Later, Morefield [58] developed a similar approach suitable for implementation. It is based upon likelihood functions and converts the association of detections to tracks into an integer programming problem. Finally, Trunk and Wilson [59] considered the effects of resolution in the track formation process.

Since the general approach of all these maximum likelihood procedures is similar, the more comprehensive approach [59] will be discussed in detail. The maximum likelihood method calculates the likelihood that a set of tracks correctly represents a given set of detections. The statement that a set of tracks represents a given set of detections means that each detection is either declared a false alarm or assigned to one or more tracks and only one detection is assigned to a track on any scan. In the calculation of the likelihood, the probability of detection, the probability of false alarm, the measurement error characteristics, and the probability of target resolution are all taken into account. For simplicity, the likelihood is only written in terms of the range measurement. Reference 59 indicates how the angle measurements are included.

The probability of obtaining N_j detections of the jth target in N_S scans is binominally distributed. Then the probability of obtaining the detections associated with a set of N_t tracks is just the product of the binomial probabilities associated with each track, i.e.,

$$\prod_{j=1}^{N_t} \binom{N_s}{N_j} P_D^{N_j}(1 - P_D)^{N_s - N_j}. \tag{53}$$

The probability of obtaining a specified number of false alarms in a range interval R_I on each of the N_s scans is given by the multinomial probability

$$N_s! \prod_{i=1}^{N_D} (P_i^{M_i}/M_i!), \tag{54}$$

where N_D is the total number of detections, M_i is the number of scans that contain exactly i false alarms, and P_i is the Poisson probability of obtaining i false alarms on any scan, i.e.,

$$P_i = (\lambda R_I)^i \exp(-\lambda R_I)/i! \tag{55}$$

where λ is the false alarm rate per unit length. Finally, the probability of a false alarm occurring at a particular range is given by the uniform density. Consequently the likelihood of a specified set of false alarms is obtained by multiplying Eq. (54) by

$$(1/R_I) \sum_{i=1}^{N_D} i\, M_i. \tag{56}$$

The likelihood of obtaining a given set of measurements on the jth track is

$$\prod_{i=2}^{N_S - 1} f[X_j(i), X_{\text{true}}(i)]/(R_I)^2 (2\pi\sigma^2)^{(N-2)/2}, \tag{57}$$

where σ^2 is the measurement error variance, $X_j(i)$ is the range of the associated detection on the ith scan, $X_{\text{true}}(i)$ is the true range of the track on the ith scan, and the function $f(\cdot,\cdot)$ is defined by

$$f(x, y) = \begin{cases} 1, & \text{if there is no detection associated with track on } i\text{th scan or if the associated detection is also associated with any other track} \\ \exp[-(x - y)^2/2\sigma^2], & \text{otherwise.} \end{cases} \tag{58}$$

The rationale behind Eq. (57) is as follows. The detections occurring on the earliest and latest scan, which may not be the first and the last scans, can occur anywhere in the range interval R_I, this in essence establishes an a priori velocity distribution. Hence, the factor $(1/R_I)^2$ reflects the uniform distribution of the first and last detections. The other detections are Gaussian distributed with mean value equal to the true position and a variance of σ^2. Since the true positions are unknown, the obvious approach is to replace the true positions by the minimum mean square estimate $\{\hat{X}_j(k)\}$. To avoid a bias caused by the estimation procedure, it was shown [59] that the initial and final error measurements should be included in Eq. (57). Consequently, one should use

$$\prod_{i=1}^{N_t} f[X_j(i), \hat{X}_j(i)/(R_I)^2\ (2\pi\sigma^2)^{[N_t-2)/2]} \tag{59}$$

instead of Eq. (57).

When several targets are close to one another, merging algorithms may yield a single detection from the closely spaced targets [35] The probability of obtaining a single, unresolved, detection X_k from N_k closely spaced targets is calculated by first ordering the predicted positions so that

$$\hat{X}_{i_1} \le \hat{X}_{i_2} \le \cdots \le \hat{X}_{i_{N_t}}$$

where for notational convenience the scan identifier has been dropped. Letting $D_m = \hat{X}_{i_m} - \hat{X}_{i_{m-1}}$, the probability of not resolving the N_k targets is given by

$$P_R(X_k) = \prod_{m=2}^{N_t} P(D_m), \tag{60}$$

where the probability of not resolving two targets separated by distance D is given in Ref. 35 by

$$P(D) = \begin{cases} 1, & D \le 1.7R \\ (2.6R - D)/0.9R, & 1.7R \le D \le 2.6R \\ 0, & D \le 2.6R \end{cases} \tag{61}$$

where R is the 3 dB pulsewidth (range cell dimension). It was shown that the density of the position of X_k can be approximated by

$$P_p(X_k) = [1/(2\pi\sigma^2)^{1/2}]\, P_E(X_k), \tag{62}$$

where

$$P_E(X_k) = [\exp(-\epsilon_k^2/2\sigma^2]/\max[1,(\hat{X}_{i_{N_s}} - \hat{X}_{i_1})/(2\pi\sigma^2)^{1/2}], \tag{63}$$

and

$$\epsilon_k = \max(0,\, X_k - \hat{X}_{i_{N_s}},\, \hat{X}_{i_1} - X_k) \tag{64}$$

is the distance from X_k to the nearest predicted position if X_k lies outside of the interval defined by the predicted positions; otherwise ϵ_k is zero. Since the factor $(2\pi\sigma^2)^{1/2}$ in Eq. (62) is already included in Eq. (59), the probability associated with unresolved detections is found by multiplying Eq. (60) and Eq. (63).

The final term in the likelihood includes the a priori probability of having N_T tracks in the local region. Since in some situations this can be the result of a deterministic decision (e.g., a wing of aircraft in a military situation), the a priori probabilities will be assumed to be equal rather than the commonly used Poisson arrival model [56,57]. In applying the method, any a priori probability appropriate to the problem of interest can be used.

In terms of the previous expressions, the likelihood of an N_T track combination is given by

$$L(N_T) = \left[\prod_{j=1}^{N_T} \binom{N_s}{N_j} P_D{}^{N_j}(1 - P_D)^{N_s - N_j} \right]$$

$$\cdot \left\{ (1/R_I) \left(\sum_{i=1}^{N_D} i\, M_i \right) N_s! \prod_{i=1}^{N_D} \left[(\lambda R_I)^{iM_i}\, e^{-\lambda M_i R_I}/M_i!\, (i!)^{M_i} \right] \right\}$$

$$\cdot \left[\prod_{j=1}^{N_T} \left\{ \prod_{i=1}^{N_s} f[(X_j(i),\, X_j(i)]/(R_I)^2\, (2\pi\sigma^2)^{(N_s-2)/2} \right\} \right]$$

$$\cdot \left[\prod_{k=1}^{N_u} P_R(X_k) P_E(X_k) \right], \tag{65}$$

where N_u is the number of unresolved detections.

Figure 35 shows an example of this procedure applied to recorded data of a flight of five aircraft. The five tracks identified are (1, M, 1, 1, M, 1), (M, 1, 2, 2, 1, 2), (2, 2, 2, M, 1, 2), (3, 3, 3, 3, 2, 3), and (4, 4, 4, 4, 3, 4); each track is represented by a sextuple with the number specifying a detection number and an M specifying a miss. We note that tracks 2 and 3 have common detections on scans 3, 5, and 6. Using Eq. (65), this sequence of tracks was over 100 times more likely than the best four track combination.

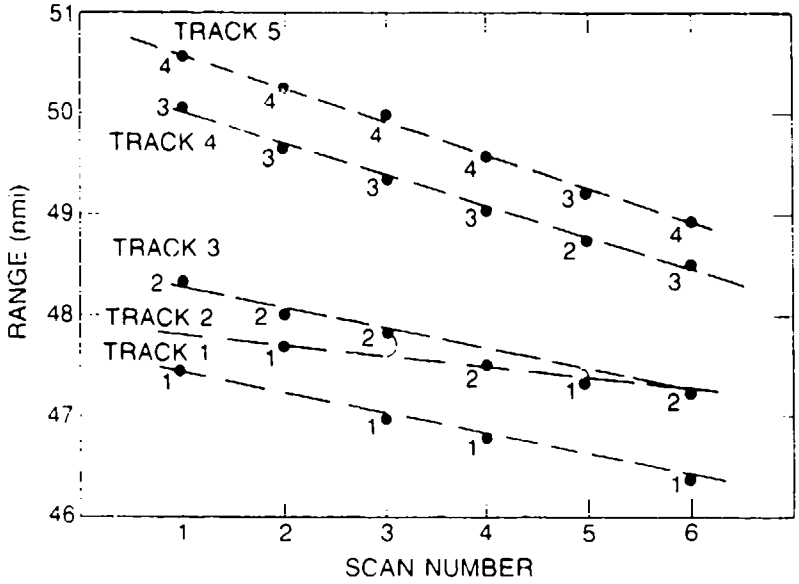

Fig. 35 — Detections per scan shown vs range. Dots indicate detections, arcs indicate unresolved detections, and lines indicate the maximum likelihood tracks.

MULTISENSOR INTEGRATION

Multisensor integration will be divided into three topics: (1) colocated radar integration, (2) multisite radar integration, and (3) integration of data from unlike sensors (e.g., radar and IFF). In this section, radars will be considered to be colocated if it is not necessary to take into account that the radars are located at different sites.

There are several methods for integrating data from multiple radars into a single system track file. The type of radar integration that should be used is a function of the radar's performance, the environment, and whether or not the radars are colocated. The several integration methods that have been used in various systems are:

- *Track Selection*

  Generate a track with each radar and choose one of the tracks as the system track.

- *Average Track*

  Generate a track with each radar and weight according to the Kalman filter's covariance matrices the individual tracks to form a system track.

- *Augmented Track*

  Generate a track with each radar, choose one of the tracks as the system track, and use selected detections from the other radars to update the system track.

- *Detection-to-Track*

  Use all radar detections to update the system track; tracks may or may not be initiated using all detections from all radars.

Theoretically, the detection-to-track method of integration yields the best tracks because all the available information is used. However, the detections must be weighted properly and care must be taken so that bad data do not corrupt good data.

There are many advantages in radar integration. Probably the most important is that it provides a common surveillance picture to all users so that decisions can be made more effectively. Radar integration will also improve track continuity and tracking on maneuvering targets because of the higher effective data rate. Improvement in track initiation times is a function of the target trajectory. For instance, long-range targets are usually detected by only one radar so that little or no improvement in initiation time is achieved. However, there could be an appreciable reduction in the initiation time for pop-up targets. Finally, the general tracking performance is improved in an ECM environment because of the integration of radars in different frequency bands located at different positions—providing both spatial and frequency diversity.

The main advantage of integrating different sensors with radar is that it provides classification and/or identification information on radar tracks. In general, the other sensors do not provide position data of accuracy comparable to the radar data. In addition to providing classification information, the sensors can alert each other of conditions that can cause the mode of operation to be changed. For instance, a strong direction finding (DF) bearing strobe that cannot be correlated with any radar track, may cause the radar to use burn through, to lower its detection thresholds, or to change its initiation criterion in the sector containing the DF bearing strobe.

The next three sections describe colocated radar integration, multisite radar integration, and unlike sensor integration.

Colocated Radar Integration

The fundamental work [37,60,61] on colocated radar integration has been performed for the U.S. Navy; typically, with a naval ship that has two or three radars within several hundred feet of one another. Although various radar integration techniques have been investigated, the one implemented on most naval ships is the detection-to-track integration philosophy. Starting with the DDG-2:15 class of ships [60,61] the U.S. Navy started placing Integrated Automatic Detection and Tracking (IADT) systems aboard various classes of U.S. Navy ships.

Figure 36 shows the typical functions of an IADT employing the detection-to-track integration philosophy. An automatic detector that performs a thresholding operation to control the false alarm rate is associated with each radar. After detections (contacts) have been declared, some further tests (contact entry logic) are applied to see whether the detections should be made available to the tracking system or discarded. For instance, a detection falling within a tracking gate is never discarded, while a detection within an area that has been declared to be land clutter is discarded if its amplitude is too large. (For a fuller description of the contact entry logic see the section entitled Contact Entry Logic.) As detections become available to the tracking system, in turn they are associated with the stationary-track filter (clutter map), the track file, and the saved detection file (previously uncorrelated detections). Thus, a detection from one radar can be correlated with a saved detection from another radar, resulting in a track entry sooner than possible from any individual radar.

The tracking algorithms for a multiple radar tracking system are quite similar to those for a single radar tracking system. Consequently, we will discuss only the difference.

First, a time is associated with each detection; then, the detection with the oldest detection time is subjected to the correlation process. In a single radar tracking system, time is not required since all the timing can take place in terms of the radar s. an time.

The second difference is that the tracking filter updates the target tracks with detections whose accuracy varies with the radar and that arrive "randomly" in time. The optimal tracking filter (with

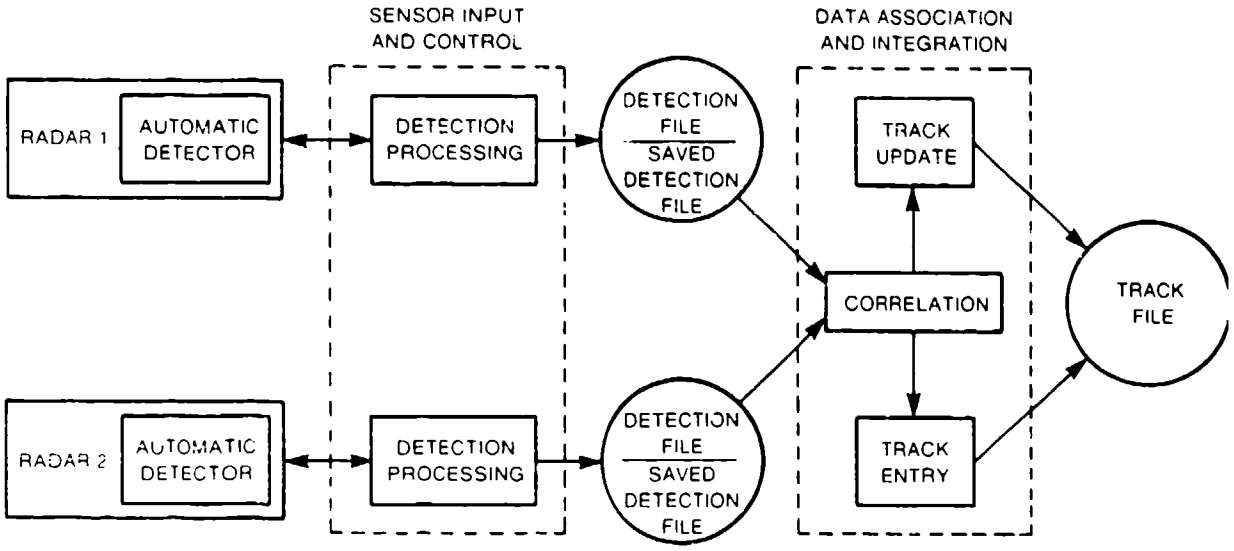

Fig. 36 — Detection-to-track processing, (copyright 1977, IEEE).
From, P.G. Casner, Jr., and R.J. Prengaman [60]

respect to the minimum mean square error) is the Kalman filter [41,42]. Consequently, either a Kalman filter or an approximation of it should be used.

Another problem unique to the multiradar tracking system is the azimuthal and range alignment between radars. This problem is solved by adaptively aligning all the radars to the 3-D radar that is arbitrarily selected to be the accurate radar. This is accomplished by examining the radar tracks that are being updated by multiple radars and that meet other specified criteria (e.g., frequency of update). Then the average error for the ith radar, over all targets between the measured and predicted position, is weighted and subtracted from future measurements made by the ith radar, over all targets. This feedback arrangement will drive the bias errors toward zero. The residue bias error is approximately 1/10 the accuracy of the measurement and prediction errors [60,61].

Multi-Site Radar Integration

The methods used for exchanging tracking information between noncolocated sites are a function of whether the sites are fixed or mobile and what communication links are available.

The most common multiple site tracking system philosophy is that one site controls a radar track (has reporting responsibility), transmits the tracking parameters over the communication link, and receiving units display the remote track. The track receives only updates from one site and thus does not benefit from the mutual support available from other radars in different frequencies and spatial location. This philosophy is usually used in any multisite system when the communication link has limited capacity.

Multisite integration with large gridlock and sensor misalignment errors is a difficult problem. If the targets from the multiple sites can be correlated, then one can use the Kalman filtering techniques to estimate the gridlock and misalignment errors [62]. However, if the gridlock and misalignment errors are large, one cannot perform the necessary correlation. Bath [63] solved this problem by solving the correlation, gridlock, and misalignment problems simultaneously. The maximum errors in latitude, longitude, and azimuth misalignment must first be defined. Next, one must define error bins of size Δx in latitude, Δy in longitude, by $\Delta\theta$ in azimuth and divide the error space into error bins of this size. The error between one track from site 1 and one track from site 2 is calculated, and a "one" is entered into the bin corresponding to the calculated error. If there are n tracks

at site 1 and m tracks at site 2, $m \times n$ errors are calculated and $m \times n$ ones are entered into the error bins. For tracks that are different, the ones will be randomly distributed throughout the error space. However, for tracks that are the same, all the ones will appear in the same error cell. An example of this two-dimensional cross-correlation function is shown in Fig. 37 where the azimuth error is zero. The spike not only gives the gridlock biases but also identifies the proper correlation of tracks from multiple sites. Kalman filter techniques could be used with the correlated track pairs to obtain more accurate estimates of the biases.

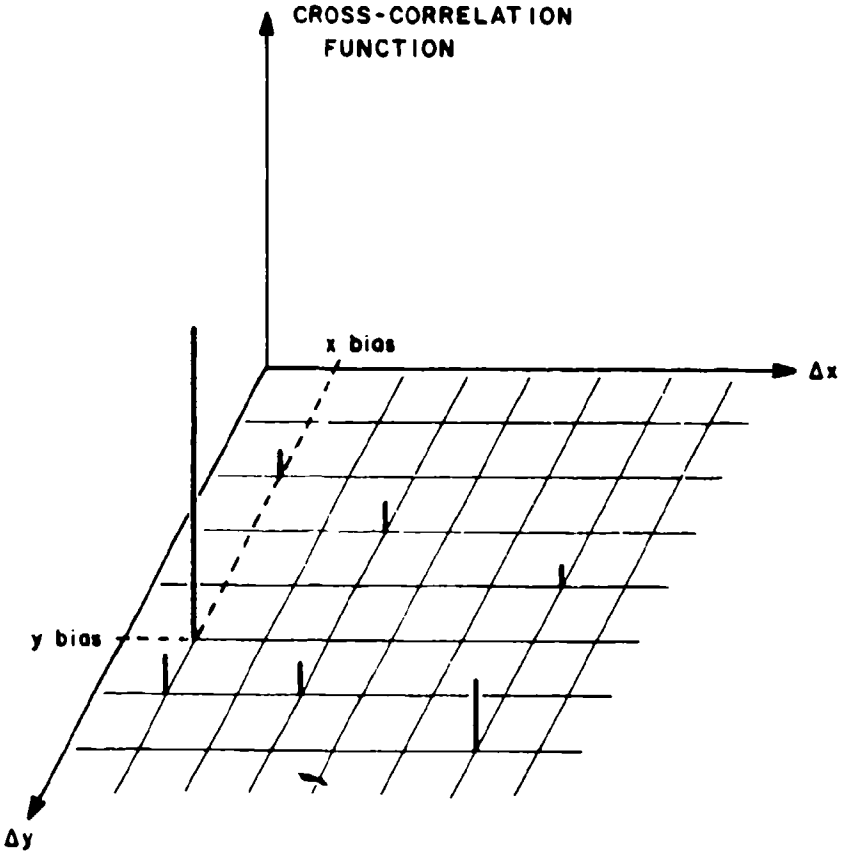

Fig. 37 — Two-dimensional cross-correlation function (for two track bases with x and y biases only). From W.G. Bath [63]

The netted radar program NRP [64] is a netted radar system for ground-target surveillance developed at the Lincoln Laboratory under the sponsorship of the U.S. Army and the Defense Advanced Research Projects Agency (DARPA). The basic idea is to associate automatic detection and tracking systems (similar to the MTD system) with each radar and then transmit tracks to a central location (Radar Control Center) where the tracks are integrated into a single track file. Tracks are transmitted rather than detections because the bandwidth required to transfer tracks is significantly lower than that required to transfer detections. The bandwidth used in the NRP system is approximately 2400 baud. The NRP system was tested at Fort Sill, Oklahoma. The automatic integration at the Radar Control Center provided continuity in track updating and identity despite missing detections caused by terrain masking and occasional misses caused by a variety of sources. Note that gridlock was obtained by surveying the radar sites. This is the usual and preferred solution to gridlock when the sites are fixed and there are time and resources to perform the survey.

The communication link is one of the keys to a successful multisite integration system. This is not a problem for traffic control and land-based air defense systems that can use telephone lines; however, it can be a problem for other systems. Usually communication links are not adequate to transmit all the useful data that are available at the sensor. A very effective alternate way of transmitting data is by means of the radar. By using the radar transmitter and antenna, essentially jam-proof communications can be established [65].

Unlike Sensor Integration

A number of sensors can be integrated: radar, IFF, IR, optical, and acoustic. However, although there has been much talk and several programs in sensor integration, there has been very little progress made. Electromagnetic sensors such as radar, IFF, and strobe extractors appear to be most easily integrated.

IFF Integration

The problem of integrating radar and IFF data is less difficult than that of integrating two radars. The question of whether detections or tracks should be integrated is a function of the application. In a military situation, by integrating detections, one could interrogate the target only a few times, identify it, and then associate it with a radar track. From then on, there would be little need for reinterrogating the target. However, if tracks were integrated, targets would be interrogated many times resulting in possibly revealing their position. However, in an air traffic situation, targets would be interrogated every scan and consequently either detections or tracks can be integrated.

Radar-DF Bearing Strobe Integration

Coleman [66] and later Trunk and Wilson [67,68] considered the problem of correlating radar tracks with DF bearing strobes. Trunk and Wilson considered the problem of given K DF angle tracks, each specified by a different number of DF measurements, associate each DF track with either no radar track or one of m radar tracks, again each radar track being specified by a different number of radar measurements. Since each target can carry multiple emitters, i.e., multiple DF tracks can be associated with each radar track, each DF track association can be considered by itself, thus resulting in K disjoint association problems. Consequently, an equivalent problem is: given a DF track specified by n DF bearing measurements, associate the DF track with no radar track or one of m radar tracks, the jth radar track being specified by m_j radar measurements. Thus, the problem reduces to the multiple hypothesis testing problem.

H_0: DF measurements associate with no radar track

H_j: DF measurements associate with jth radar track.

Using a combination of Bayes and Neyman Pearson procedures and assuming that the DF measurements errors are usually independent and Gaussian distributed with zero mean and constant variance σ^2 but with occasional outliers (i.e., large errors, not described by the Gaussian density), they argued that the decision should be based on the probability

$$P_j = \text{Probability}\,(Z \geq d_j)\,, \tag{66}$$

where Z has a chi-square density with n_j degrees of freedom and d_j is given by

$$d_j = \sum_{i=1}^{n} \text{Min}\{4,\ [\theta_e(t_i) - \theta_j(t_i)]^2/\sigma^2\} \qquad j = 1, \ldots, m\,, \tag{67}$$

where n_j is the number of DF measurements overlapping the time interval for which the jth radar track exists, $\theta_e(t_i)$ is the DF measurement at time t_i, $\theta_j(t_i)$ is the predicted azimuth of radar track j for time t_i, and the factor 4 limits the square error to $4\sigma^2$ to account for DF outliers. Using the largest P_j's designated $P_{\max}$ and P_{next} and thresholds T_L, T_H, T_M, and R, the following decision rule was generated

Firm Correlation: $P_{\max} \geq T_H$ and $P_{\max} \geq P_{next} + R$;

Tentative Correlation: $T_H > P_{\max} \geq T_M$ and $P_{\max} \geq P_{next} + R$;

Tentative Correlation with Some Track: $P_{\max} \geq T_M$ but $P_{\max} < P_{next} + R$;

Tentatively Uncorreiated: $T_M > P_{\max} > T_L$; and

Firmly Uncorrelated: $T_L \geq P_{\max}$,

where the decision means the following:

Firm Correlation, DF signal goes with the radar track that has the largest P_j (i.e., $P_{\max}$)

Tentative Correlation, DF signal probably goes with the radar track that has the largest P_j (i.e., $P_{\max}$)

Tentative Correlation with Some Track, DF signal probably goes with some radar track, but it cannot determine which

Tentatively Uncorrelated, DF signal probably does not go with any radar track

Firmly Uncorrelated, DF signal does not go with any radar track.

The lower threshold T_L determines the probability that the correct radar track (i.e., the one associated with the DF signal) will be incorrectly rejected from further consideration. This threshold is set by noting that the probability P_j for the correctly associated radar track is uniformly distributed between zero and one. Thus, if one desires to keep the rejection rate for the correct track below P_R, one can obtain this by setting $T_L = P_R$. The threshold T_H is set equal to P_{FA} defined as the probability of falsely associating a radar track with a DF signal when the DF signal does not belong with the radar track. The threshold T_H is a function of the azimuth difference μ between the true (DF) position and the radar track under consideration. The threshold T_H was found for the $\mu = 1.0\ \sigma$ and $\mu = 1.5\ \sigma$ by simulation techniques, and the results for $P_{fa} = 0.01$ are shown in Fig. 38. Between the high and low thresholds there is a tentative region. The middle threshold divides the "tentative" region into a tentative-correlated region and a tentatively uncorrelated region. The rationale in setting the threshold is to set the two associated error probabilities equal for a particular separation; i.e., $Pr\{P_j \leq T_M \mid \text{correct match}\} = Pr\{P_j \geq T_M \mid \text{incorrect match}\}$. The threshold T_M was found by using simulation techniques and is shown in Fig. 39.

The purpose of the probability margin R is to ensure the selection of the proper DF-radar association (avoiding false target classifications) when there are two or more radar tracks close to one another. The correct selection is reached by postponing a decision until the two discriminant probabilities differ by R. The value for R is found by specifying a probability of an association error P_e according to $P_e = P_R\{P_{\max} \geq P_{next} + R\}$, where $P_{\max}$ corresponds to an incorrect association and P_{next} corresponds to the correct association. The probability margin R is a function of P_e and the

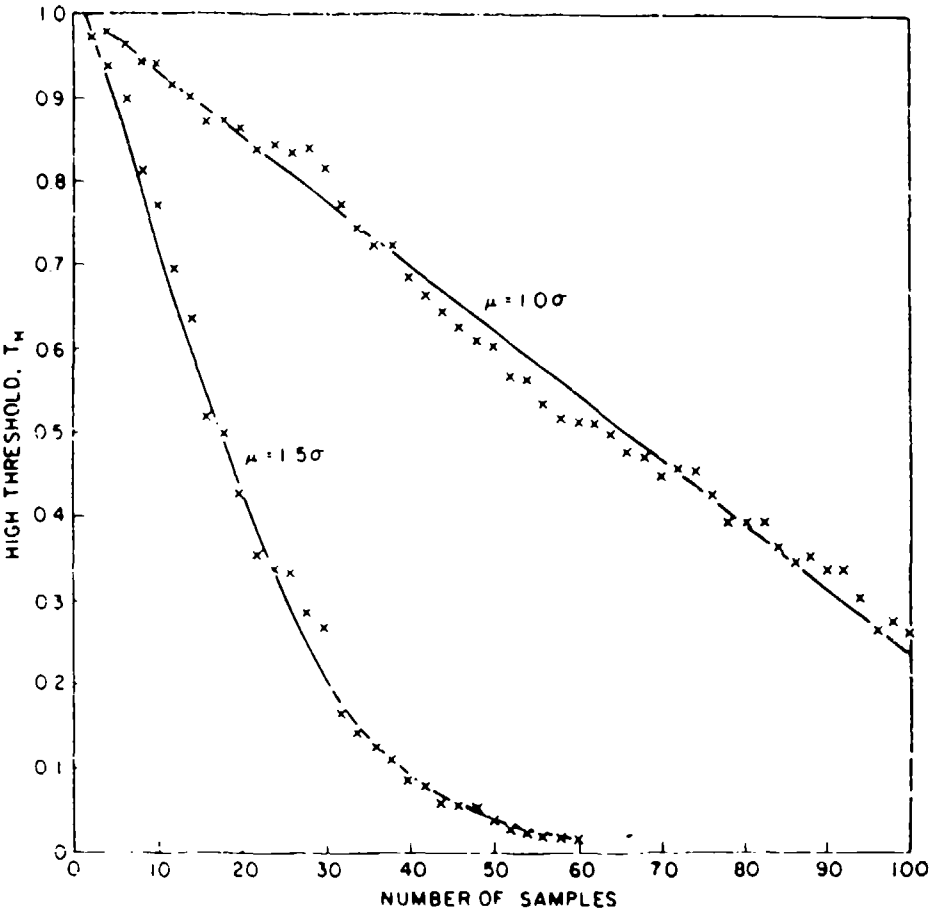

Fig. 38 — High threshold vs number of samples for two different separations. The x's are the simulation results, (copyright 1987, IEEE). From G.V. Trunk and J.D. Wilson [67]

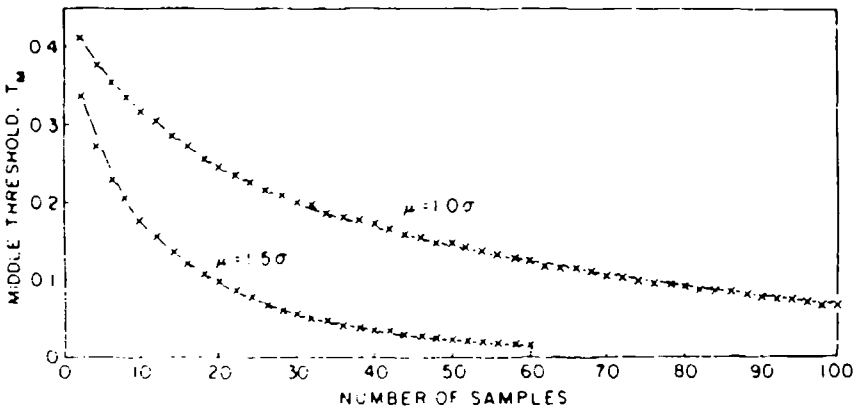

Fig. 39 — Middle threshold vs number of samples for two different target separations. The x's are the simulation results, (copyright 1987, IEEE). From G.V. Trunk and J.D. Wilson [67]

separation μ of the radar tracks. The probability margin R was found for $\mu = 0.25\ \sigma$, $0.50\ \sigma$, and $1.00\ \sigma$ by using simulation techniques, and Fig. 40 shows the results for $P_e = 0.01$. Since the curves cross one another, we can ensure that $P_e \leq 0.01$ for any μ by setting R equal to the maximum value of any curve for each value of n.

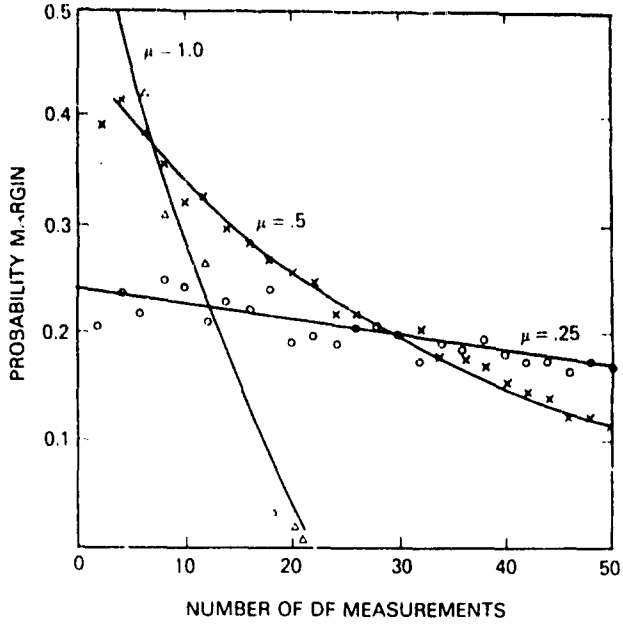

Fig. 40 — Probability margin vs number of DF measurements for three different target separations. The O's, ×'s and Δ's are the simulation results for $\mu = 0.25$, $\mu = 0.5$, and $\mu = 1.0$, respectively, (copyright 1987, IEEE). From G.V. Trunk and J.D. Wilson [67]

The algorithm was evaluated by using simulations and recorded data. When the radar tracks are separated by several standard deviations of the measurement error, correct decisions are rapidly made. However, if the radar tracks are close to one another, errors are avoided by postponing the decision until sufficient data are accumulated. An interesting example is shown in Figs. 41 through 43. Figure 41 shows the radar (azimuth) measurements of the control aircraft, the radar measurements of four aircraft of opportunity in the vicinity of the control aircraft, and the DF measurements from the radar on the control aircraft. The probability discriminants, one without limiting, the other with limiting, are shown in Figs. 42 and 43, respectively. Initially, an aircraft of opportunity has the highest discriminant probability; however, a firm decision is not made since P_{max} does not exceed P_{next} by the probability margin. After the 14th DF measurement, the emitter is firmly correlated with the control aircraft. However, at the 18th DF measurement, a very bad measurement is made (outlier) and the firm correlation is downgraded to a tentative correlation. Figure 43 shows that, if limiting is employed, the correct decision remains firm.

In a complex environment where there are many radar tracks and DF signal sources, it is quite possible that many DF signals will be assigned the category that the DF signal probably goes with some radar track. To remove many of these ambiguities, multiple-platform DF operation can be considered. The extension of the previous procedures to multiple-platform operation is straightforward. Specifically, if $\theta_{e1}(t_i)$ and $\theta_{e2}(t_k)$ are the DF angle measurements with respect to platforms 1 and 2,

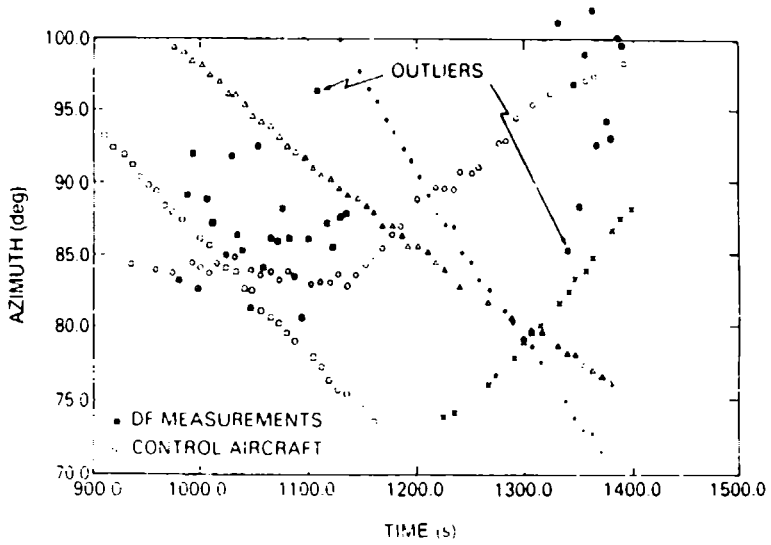

Fig. 41 — Radar detections o and DF measurements collected on the control aircraft. The ○'s, Δ's +'s, and ×'s are radar detections on four aircraft of opportunity in the vicinity of the control aircraft, (copyright 1987, IEEE). From G.V. Trunk and J.D. Wilson [67]

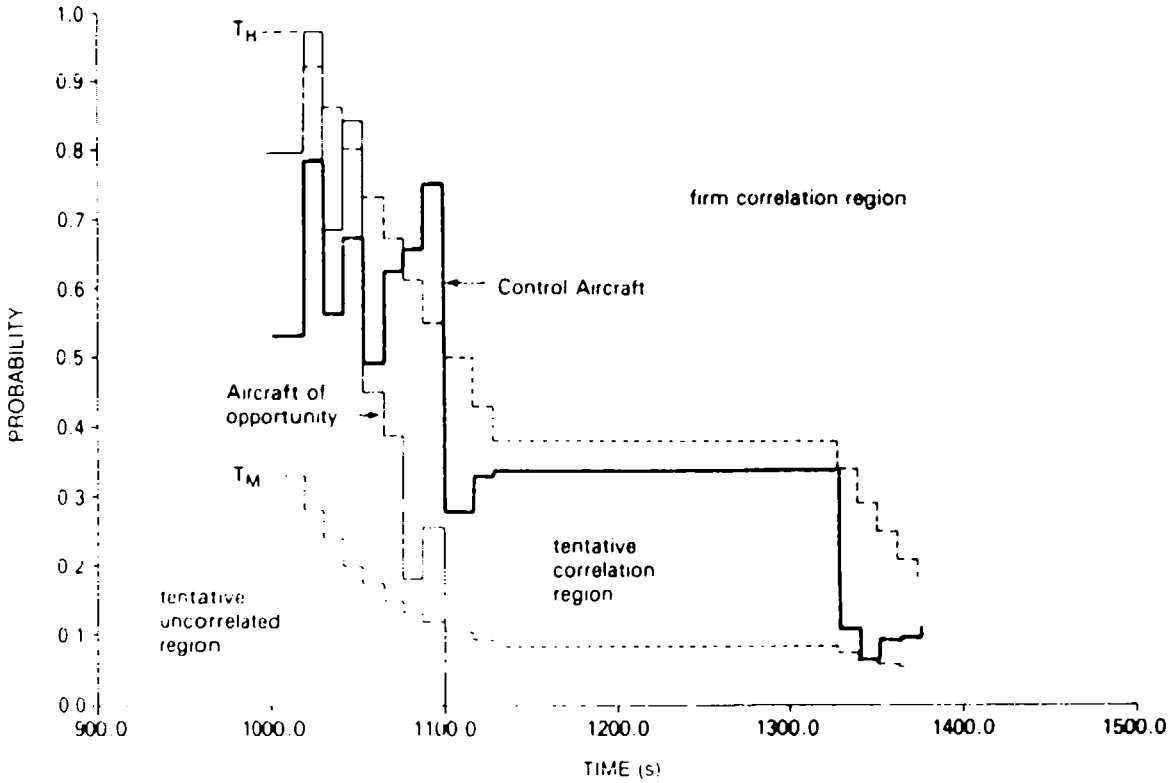

Fig. 42 — Probability discriminant for experimental data: solid line is discriminant, and dashed lines are thresholds T_M and T_H. No limiting used, (copyright 1987, IEEE). From G.V. Trunk ad J.D. Wilson [67]

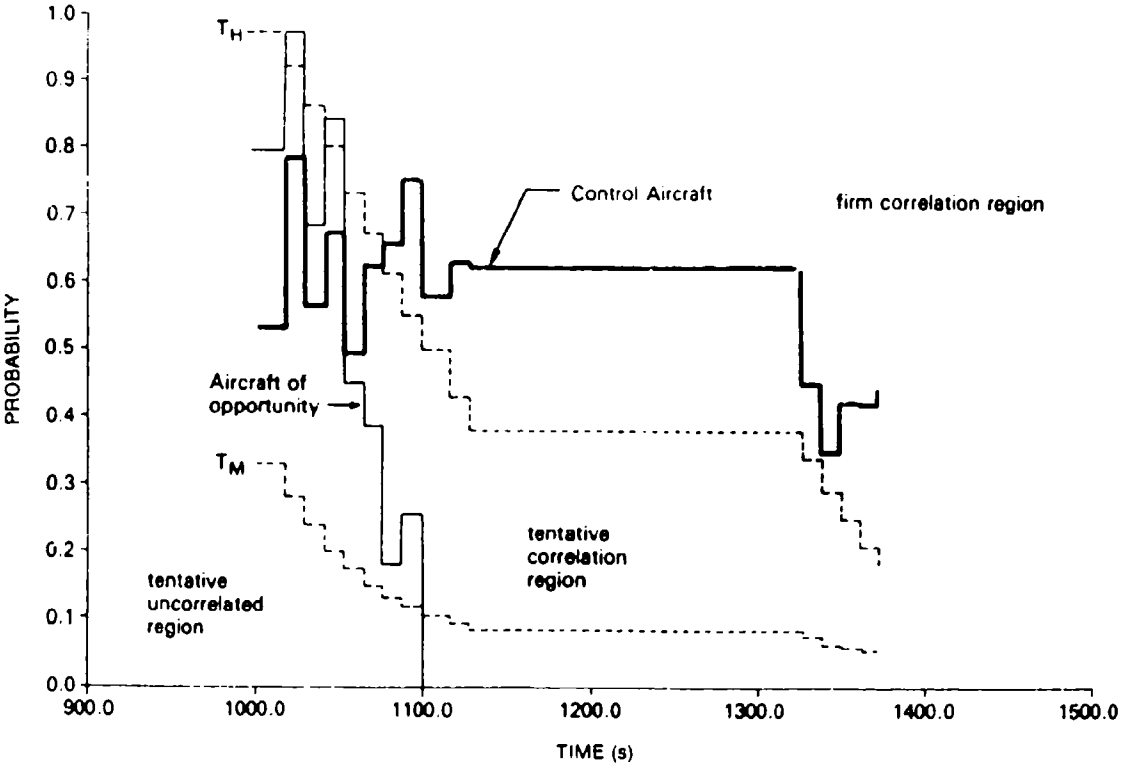

Fig. 43 — Probability discriminant for experimental data: solid line is discriminant, and dashed lines are thresholds T_M and T_H. Limiting used, (copyright 1987, IEEE). From G.V. Trunk and J.D. Wilson [67]

and $\theta_{j1}(t_i)$ and $\theta_{j2}(t_k)$ are the estimated angular positions of radar track j with respect to platforms 1 and 2, the multiplatform square error is simply

$$d_j = \sum_{i=1}^{n_{1j}} \text{Min}\,\{4, [\theta_{e1}(t_i) - \theta_{j1}(t_i)]^2/\sigma_1^2\}$$

$$+ \sum_{k=1}^{n_{2j}} \text{Min}\,\{4, [\theta_{e2}(t_k) - \theta_{j2}(t_k)]^2/\sigma_2^2\}. \tag{68}$$

Then, the previously described procedure can be used with d_j being defined by Eq. (68) instead of Eq. (67).

REFERENCES

1. J.I. Marcum, "A Statistical Theory of Target Detection by Pulsed Radar," *IRE Trans. Info. Theory* **6**, 59-267 (1960).

2. P. Swerling, "Probability of Detection for Fluctuating Targets," *IRE Trans. Info. Theory* **6**, 269-308 (1960).

3. J. Neyman and E.S. Pearson, "On the Problems of the Most Efficient Tests of Statistical Hypotheses," *Philos. Trans. R. Soc. London*, Series A **231**, 289-337 (1933).

4. L.V. Blake, "The Effective Number of Pulses per Beamwidth for a Scanning Radar," *Proc IRE* **41**, 770-774 (1953).

5. G.V. Trunk, "Comparison of the Collapsing Losses in Linear and Square-Law Detectors," *Proc. IEEE* **60** (6), 743-744 (1972).

6. P. Swerling, "Maximum Angular Accuracy of a Pulsed Search Radar," *Proc. IRE* **44**, 1146-1155 (1956).

7. G.V. Trunk, "Survey of Radar ADT," NRL Report 8698, Jun 1983.

8. D.C. Cooper and J.W.R. Griffiths, "Video Integration in Radar and Sonar Systems," *J. British IRE* **21**, 421-433 (1961).

9. V.G. Hansen, "Performance of the Analog Moving Window Detector," *IEEE Trans. Aerospace and Electronic Systems* **AES-6**, 173-179 (1970).

10. G.V. Trunk, "Comparison of Two Scanning Radar Detectors: the Moving Window and the Feedback Integrator," *IEEE Trans. Aerospace and Electronic Systems* **AES-7**, 395-398 (1971).

11. G.V. Trunk, "Detection Results for Scanning Radars Employing Feedback Integration," *IEEE Trans. Aerospace and Electronic Systems*, **AES-6**, 522-527 (1970).

12. B.H. Cantrell and G.V. Trunk, "Angular Accuracy of a Scanning Radar Employing a Two-Pole Filter," *IEEE Trans. Aerospace and Electronic Systems* **AES-9**(5), 649-653 (1973).

13. B.H. Cantrell and G.V. Trunk, "Correction to 'Angular Accuracy of a Scanning Radar Employing a Two-Pole Filter'," *IEEE Trans. Aerospace and Electronic Systems* **AES-10**(6), 878-880 (1974).

14. P. Swerling, "The 'Double Threshold' Method of Detection," Project Rand Research Memo RM-1008, Dec. 17, 1952.

15. J.V. Harrington, "An Analysis of the Detection of Repeated Signals in Noise by Binary Integration," *IRE Trans. Info. Theory* **IT-1**(1), 1-9 (1955).

16. M. Schwartz, "A Coincidence Procedure for Signal Detection," *IRE Trans. Info. Theory* **IT-2**(4), 135-139 (1956).

17. D.H. Cooper, "Binary Quantization of Signal Amplitudes: Effect for Radar Angular Accuracy," *IEEE Trans. Aerospace and Navigational Electronics* **ANE-11**, 65-72 (1964).

18. G.M. Dillard, "A Moving-Window Detector for Binary Integration," *IEEE Trans. Info. Theory* **IT-13**(1), 2-6 (1967).

19. D.C. Schleher, "Radar Detection in Log-Normal Clutter," IEEE 1975 International Radar Conference, pp. 262-267, Arlington, VA, 1975.

20. Y-H. Mao, "The Detection Performance of a Modified Moving Window Detector," *IEEE Trans. Aerospace and Electronic Systems* **AES-17**(3), 392-400 (1981).

21. Johns Hopkins University, Applied Physics Laboraroy Report FP8-T-013, "Radar Processing Subsystem Evaluation," Nov. 1975.

22. H.M. Finn and R.S. Johnson, "Adaptive Detection Mode with Threshold Control as a Function of Spacially Sampled Clutter-Level Estimates," *RCA Rev.* **29**, 414-464 (1968).

23. R.L. Mitchell and J.F. Walker, "Recursive Methods for Computing Detection Probabilities," *IEEE Trans. Aerospace and Electronic Systems* **AES-7**(4), 671-676 (1971).

24. G.V. Trunk and J.D. Wilson, "Automatic Detector for Suppression of Sidelobe Interference," 1977 IEEE Conference on Decision and Control, New Orleans, LA, Dec. 7-9, 1977, pp. 508-514.

25. G.V. Trunk and P.K. Hughes II, "Automatic Detectors for Frequency-Agile Radar," International Radar Conference, Radar-82, London, 1982, pp. 464-468.

26. G.V. Trunk, B.H. Cantrell, and F.D. Queen, "Modified Generalized Sign Test Processor for 2-D Radar," *IEEE Trans. Aerospace and Electronic Systems* **AES-10**(5), 574-582, (1974).

27. J.T. Rickard and G.M. Dillard, "Adaptive Detection Algorithms for Multiple-Target Situations," *IEEE Trans. Aerospace and Electronic Systems* **AES-13**(4), 338-343 (1977).

28. B.A. Green, "Radar Detection Probability with Logarithmic Detectors," *IRE Trans. Info. Theory* **IT-4**, 50-52 (1958).

29. V.G. Hansen and J.R. Ward, "Detection Performance of the Cell Averaging Log/CFAR Receiver," *IEEE Trans. Aerospace and Electronic Systems* **AES-8**(5), 648-652 (1972).

30. G.M. Dillard and C.E. Antoniak, "A Practical Distribution-Free Detection Procedure for Multiple-Range-Bin Radars," *IEEE Trans. Aerospace and Electronic Systems* **AES-6**(5), 629-635 (1970).

31. V.G. Hansen and B.A. Olsen, "Nonparametric Radar Extraction Using a Generalized Sign Test," *IEEE Trans. Aerospace and Electronic Systems* **AES-7**(5), 942-950 (1971).

32. V.G. Hansen, "Detection Performance of Some Nonparametric Rank Tests and an Application to Radar," *IEEE Trans. Information Theory* **IT-16**(3), 309-318, (1970).

33. W.G. Bath, L.A. Biddison, S.F. Haase, and E.C. Wetzlar, "False Alarm Control in Automated Radar Surveillance Systems," 1982 International Radar Conference, Radar-82, London, 1982, pp. 71 75.

34. C.E. Muehe, L. Cartledge, W.H. Drury, E.M. Hofstetter, M. Labitt, P.B. McCorison, and V.J. Sferrino, "New Techniques Applied to Air-Traffic Control Radars," *Proc. IEEE* **62**, 716-723 (1974).

35. G.V. Trunk, "Range Resolution of Targets Using Automatic Detectors," *IEEE Trans. Aerospace and Electronic Systems* **AES-14**(5), 750-755 (1978).

36. G.V. Trunk, "Range Resolution of Targets," *IEEE Trans. Aerospace and Electronic Systems*, **AES-20**(6), 789-797 (1984).

37. B.H. Cantrell, G.V. Trunk, F.D. Queen, J.D. Wilson, and J.J. Alter, "Automatic Detection and Integrated Tracking System," IEEE 1975 International Radar Conference, Washington, DC, 1975, pp. 391-395.

38. B.H. Cantrell, G.V. Trunk, and J.D. Wilson, "Tracking System for Two Asynchronously Scanning Radars," NRL Report 7841, Dec. 1974.

39. B.H. Cantrell, "Description of an α-β Filter in Cartesian Coordinates," NRL Report 7548, Mar. 1973.

40. A.L. Quigley and J.E. Holmes, "The Development of Algorithms for the Formation and Updating of Tracks," Admiralty Surface Weapons Establishment, ASWE-WP-XBC-7512, Portsmouth P06 4AA, Nov. 1975.

41. R.E. Kalman, "A New Approach to Linear Filtering and Prediction Problems," *J. Basic Eng. ASME Trans. Ser. D* **82**, 35-45 (1960).

42. R.E. Kalman and R.S. Bucy, "New Results in Linear Filtering and Prediction Theory," *J. of Basic Eng. ASME Trans. Ser. D* **83**, 95-108 (1961).

43. A.L.C. Quigley, "Tracking and Associate Problems," IEEE International Conference on Radar—Present and Future, London, 1973, pp. 352-357.

44. T.R. Benedict and G.W. Bordner, "Synthesis of an Optimal Set of Radar Track-While-Scan Smoothing Equations," *IRE Trans. Automatic Control* **AC-7**(4), 27-32 (1962).

45. B.H. Cantrell, "Behavior of α-β Tracker for Maneuvering Target Under Noise, False Target, and Fade Conditions," NRL Report 7434, Aug. 1972.

46. A.L. Quigley and J.E. Holmes, "The Development of Algorithms for the Formation and Updating of Tracks," Admiralty Surface Weapons Establishment, WP-XBC-7512, Portsmouth P06 4AA, Nov. 1975.

47. R.A. Singer, "Estimating Optimal Tracking Filter Performance for Manned Maneuvering Targets," *IEEE Trans. Aerospace and Electronic Systems* **AES-6**(4), 473-484 (1970).

48. R.J. Prengaman, R.E. Thurber, and W.B. Bath, "A Retrospective Detection Algorithm for Extraction of Weak Targets in Clutter and Interference Environments," 1982 International Radar Conference, Radar-82, London, 1982, pp. 341-345.

49. S.R. Cook, "Development of IADT Tracking Algorithm," Johns Hopkins Univ., Applied Physics Laboratory F3C-1-061, Sept. 1974.

50. R.A. Singer and R.G. Sea, "New Results in Optimizing Surveillance System Tracking and Data Correlation Performance in Dense Multitarget Environments," *IEEE Trans. Automatic Control* **AC-18**, 571-581 (1973).

51. R.A. Singer, R.G. Sea, and K.B. Housewright, "Derivation and Evaluation of Improved Tracking Filters for Use in Dense Multitarget Environments," *IEEE Information Theory* **IT-20**(4), 423-432 (1974).

52. Y. Bar-Shalom and A. Jaffer, "Adaptive Nonlinear Filtering for Tracking with Measurements of Uncertain Origin," Proc. 1972 IEEE Conf. Decision and Control, New Orleans, LA, Dec. 1972, pp. 243-247.

53. Y. Bar-Shalom and E. Tse, "Tracking in a Cluttered Environment with Probabilistic Data Association," Proc. 4th Symp. Nonlinear Estimation, Univ. CA, San Diego, Sept. 1973, pp. 13-22 and *Automatica* **11**, 1975, pp. 451-460.

54. S.B. Colegrove and J.K. Ayliffe, "An Extension of Probabilistis Data Association to Include Track Initiation and Termination," Convention Digest, 20th IREE International Convention, Melbourne, Sept. 1985, pp. 853-856.

55. S.B. Colegrove, A.W. Davis, and J.K. Ayliffe, "Track Initiation and Nearest Neighbors Incorporated into Probabilistic Data Association," *J. Electrical and Electronics Eng., Australia—IE Aust. and IREE Aust.* **6**(3), 191-198 (1986).

56. R.W. Sittler, "An Optimal Association Problem in Surveillance Theory," *IEEE Trans. Military Electronics* **MIL-8**, 125-139 (1964).

57. J.J. Stein and S.S. Blackman, "Generalized Correlation of Multitarget Track Data," *IEEE Trans. Aerospace and Electronic Systems* **AES-11**(6), 1207-1217 (1975).

58. C.L. Morefield, "Application of 0-1 Integer Programming to Multitarget Tracking Problems," *IEEE Trans. Automat. Contr.* **AC-22**, 300-310 (1977).

59. G.V. Trunk and J.D. Wilson, "Track Initiation of Occasionally Unresolved Radar Targets," *IEEE Trans. Aerospace and Electronic Systems* **AES-17**(1), 122-130 (1981).

60. P.G. Casner, Jr., and R.J. Prengaman, "Integration and Automation of Multiple Colocated Radars," EASCON 1977, Wash., DC, pp. 10-1A to 10-1E.

61. P.G. Casner and R.J. Prengaman, "Integration and Automation of Multiple Colocated Radars," Radar-1977, IEE 1977 International Radar Conference, London, 1977, pp. 145-149.

62. J.T. Miller, "Gridlock Analysis Report, Volume I: Concept Development," Johns Hopkins University, Applied Physics Laboratory FS-82-023, Feb. 1982.

63. W.G. Bath, "Association of Multiside Radar Data in the Presence of Large Navigation and Sensor Alignment Errors," IEE 1982 International Radar Conference, London, 1982, pp. 169-173.

64. M.I. Mirkin, C.E. Schwartz, and S. Spoerri, "Automated Tracking with Netted Ground Surveillance Radars," IEEE 1980 International Radar Conf., Arlington, VA, pp. 371-379.

65. B.H. Cantrell, J.O. Coleman, and G.V. Trunk, "Radar Communications," NRL Report 8515, Aug. 1981.

66. J.O. Coleman, "Discriminants for Assigning Passive Bearing Observations to Radar Targets," IEEE 1980 International Radar Conf., Arlington, VA, pp. 361-365.

67. G.V. Trunk and J.D. Wilson, "Association of DF Bearing Measurements with Radar Tracks," *IEEE Trans. Aerospace and Electronic Systems* **AES-23**(4), 438-447 (1987).

68. G.V. Trunk and J.D. Wilson, "Correlation of DF Bearing Measurements with Radar Tracks," IEE 1987 International Radar Conf., Radar-87, London, 1987.